CHALMERS

Modelling, control and investigation of an HVDC transmission for an offshore wind farm

A centralized control strategy for offshore wind farms

Master of Science Thesis in Electric Power Engineering

BAHMAN KAHINPOUR

Department of Energy and Environment
Division of Electric Power Engineering
CHALMERS UNIVERSITY OF TECHNOLOGY
Göteborg, Sweden, May 2009

THESIS FOR THE DEGREE OF MASTER OF SCIENCE

Modelling, control and investigation of an HVDC transmission for an offshore wind farm

A centralized control strategy for offshore wind farms

BAHMAN KAHINPOUR

Examiner: Prof. Torbjörn Thiringer
Supervisor: Dr. Stefan Lundberg

Department of Energy and Environment
Division of Electric Power Engineering
CHALMERS UNIVERSITY OF TECHNOLOGY
Göteborg, Sweden, May 2009

Modelling, control and investigation of an HVDC transmission for an offshore wind farm

A centralized control strategy for offshore wind farms

Department of Energy and Environment
Division of Electric Power Engineering
CHALMERS UNIVERSITY OF TECHNOLOGY
Göteborg, Sweden, May 2009

In the name of God, the Merciful, the Compassionate

Abstract

The aim of this report is to introduce the concept of a centralized control strategy for an offshore wind farm and demonstrate it as an interesting solution for the offshore wind farms through showing its feasibility, analyzing its advantages and evaluating it from an energy production point of view. In this thesis work, first of all, a model of the wind turbine including the induction generator, the non-stiff shaft with a gear-box and the wind energy conversion is derived and is implemented in MATLAB/Simulink and PSCAD/EMTDC. In the next step, a control strategy based on the induction machine V/Hz control principles is derived which is aimed to maximize the aerodynamic conversion efficiency through setting an appropriate frequency for the offshore wind farm and also to minimize the induction generator and the transformer losses through setting an appropriate voltage level for the offshore wind farm. The latter case involves decreasing the fluxes in the generators and the transformers of the wind turbines at low wind speeds in order to decrease the losses in the cores of the wind turbine generators and transformers. The derived strategy is also implemented in the both simulation software and verified. The mentioned loss minimization feature is derived with expandability in mind so that it may be a base for the future work and also may be applied in systems not related to the wind systems. The convergence of the nonlinear centralized speed control algorithm is shown in MATLAB and the effectiveness of the derived control strategy in controlling the flux and the speed is demonstrated. In addition, the losses due to the removal of an individual control system in each wind turbine is also calculated and shown as percentage of the annual wind farm production.

In the end of the report, it is concluded that in the offshore wind farms where an HVDC transmission is used, it is possible to remove the individual control systems along with the corresponding converters and replace them with a single larger converter in the HVDC station. In this case, a more advanced control strategy should be used for controlling the converter in the HVDC station. In this thesis work, it is shown that it is possible to derive a centralized control strategy. The control strategy that the controller follows should involve the maximization of the energy absorbed from the wind by the wind turbines through setting the correct reference grid frequency and thus the correct reference rotational speed for the whole wind farm and also compensate for the slip so that the aerodynamic efficiencies become maximum and also may involve minimizing the lost energy by increasing the efficiencies through setting the correct reference voltage level. It is shown in this work that the energy input to the wind turbine can be maximized by setting a correct rotational speed as the reference and the lost energy in the system can be minimized by lowering the flux magnitude at low wind speeds. It is also shown that in addition to being feasible, the percentage of the annual lost energy due to using this centralized strategy is less than 2% in the worst case and moreover such losses decrease in the areas where the wind is less gusty.

Keywords: Offshore wind farm, HVDC converter advantages, Loss minimization, Aerodynamic efficiency maximization, Optimization, Energy efficiency, Variable frequency drive.

Acknowledgements

The project was carried out in the Division of Electric Power Engineering at Chalmers University of Technology. I would like to thank all the staff and the friends in the department that helped me and cooperated with me during the thesis work. I especially would like to express my thanks to my supervisor Dr. Stefan Lundberg for his invaluable guidance and support. Furthermore, I would like to express my thanks to my examiner Prof. Torbjörn Thiringer for his precious comments and support. And in the end, I would like to express my appreciation to my dear family for their great love and support through all my life.

Table of Contents

1. Introduction

1.1. Background of the problem

There is a certain friction between the wind and the surface on which it blows. This friction brings about a specific decreasing in the wind speed which corresponds to an amount of loss of available wind energy. Moreover, this friction leads to turbulence which prevents the wind turbines from capturing the wind energy efficiently. These negative effects depend on the type of the surface on which the wind is blowing. It turns out that on the average, the sea surface has a much smoother surface than the ground, and causes less decrement in the wind speed. Hence, offshore wind farms are attractive choices in this aspect. In addition, although in some places there are truly good wind conditions making it appropriate to build a wind farm, the resources like the ground where the wind farm should be built are not readily available. Hence, the potential wind energy may not be used. However, there are fewer limits on building the wind farms far out in the sea, but on the other hand, special skills are needed in order to build an offshore wind farm. Also, the noises from the wind turbines are a problem for humans and the environment nearby. So, not all the operating conditions are possible for the wind turbine as it may cause disturbances. But, in an offshore wind farm, there are less limitations and restrictions due to the noises made.

Transferring large amounts of electric power over long distances requires a sophisticated and efficient method of transmission such as an HVDC transmission system. As the rating of an offshore wind farms increases and it gets more distant to the shore, the need for using a more sophisticated transmission such as an HVDC transmission system increases. In addition, using an HVDC transmission with voltage source converters provides the system with more stability due to the fact that the amount of active power transferred may be controlled by the HVDC link. Also, the offshore and onshore grids are isolated from each other due to the existence of the HVDC link which protects either grid from the faults on the other side. If the wind turbines are isolated from the onshore grid faults, there may be a possibility of employing them without a fault-ride-through system which simplifies the wind turbine system. Also, there will be possibility of connecting them to a weaker grid onshore. Furthermore, the voltage and frequency offshore may be manipulated by a controller in the offshore HVDC side to control the wind turbines centrally which makes it possible to remove the individual speed control systems and corresponding converters and still makes it possible to obtain a higher efficiency of the wind farm due to the possibility of having a variable rotational speed.

The interest for the wind energy is increasing and a great deal of investment is being moved towards it. There are plans for larger wind farms with higher power ratings in many countries. Because of the mentioned reasons, offshore wind farms with HVDC transmission systems may be an attractive solution for future wind farms. Figure 1.1 demonstrates the general configuration of an offshore wind farm employing an HVDC transmission system for the power transmission.

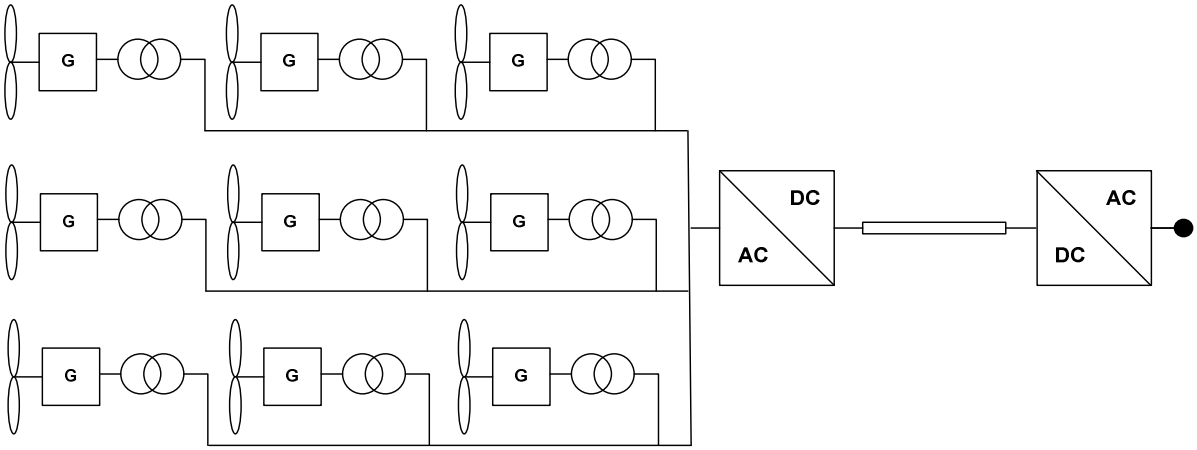

Figure 1.1 – General configuration of an offshore wind farm with an HVDC transmission

1.2. Overview of the previous works

In [1] and [2] different configurations and layouts of the offshore wind farms have been studied. The converters which are needed for offshore wind farms have been studied from an economical point of view in [3]. In these works, the advantages and disadvantages of employing an HVDC link for the energy transportation have been discussed. In [4] and [5], using an HVDC transmission for offshore wind farm applications has been demonstrated as an interesting solution. In [2] the possibility of controlling a wind farm centrally from inside the HVDC station has been shown but the feasibility of using the converter of the HVDC station to increase the efficiency of the wind turbines has not been investigated. Also, annual produced energy evaluation for such an offshore wind farm has not been done.

1.3. The purpose of the report

The purpose of this report is to determine the reference voltage and frequency of the custom grid of an offshore wind farm with an HVDC transmission based on the induction machine V/Hz control principle, wind farm loss minimization and aerodynamic efficiency maximization principles and also to implement and simulate the centralized wind farm control strategy and also evaluate it from an annual produced energy point of view.

1.4. The layout of the report

In the second chapter of this report, an introduction to the wind and its conversion and its usage in addition to some information on wind turbines, wind farms and their energy production is given. In the third chapter, the model of a wind turbine suitable for the simulations in this work is derived. The model includes an induction generator, its double-mass interface, a gear-box and the wind energy conversion mechanism. In the fourth chapter, the control strategies needed for the centralized control of an offshore wind farm are derived in detail. In the fifth chapter, the control strategies described in chapter four are actually implemented and simulated and their validity is shown and after that, they are evaluated from an annual produced energy point of view.

2. The wind turbine theory

2.1. The wind turbine system

In order to utilize the wind energy, a system is required to capture the wind energy, convert it into mechanical form and then apply it to a generator for conversion into electrical form. Figure 2.1 demonstrates the general structure of a wind turbine. Additional equipment like transformers and power electronic converters are also needed to operate a wind turbine.

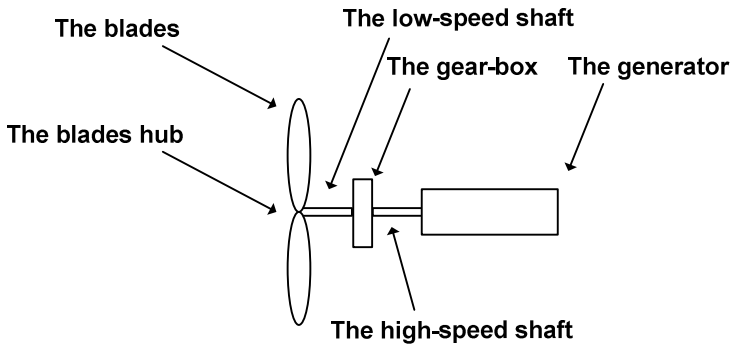

Figure 2.1 – The wind turbine system

A wind turbine generally consists of three blades connected to a central hub which is connected to a low-speed shaft. A wind turbine rotates at a low speed. Hence, a gear-box is usually needed to increase the speed up to the electrical frequency range. In the case of a very high pole-pair number, a gear-box may be avoided. The gear-box is connected to a high-speed shaft which is the shaft of a generator. Different types of generators may be used in a wind turbine which will be discussed later in the text.

Controlling the energy which is captured by the blades is necessary due to the fact that there should be a method to control and limit the converted energy as the wind speed changes. Especially, the case of high turbine speed at high wind speeds should be avoided as stopping a wind turbine may be impossible if the wind turbine speed becomes too high while there is strong wind blowing [6]. Therefore, the wind turbine speed should always be monitored and controlled and there should be a way to control the absorbed energy. One method to achieve this is to use the pitch angle control mechanism, which is the method of employing blades with turnable parts which may be turned either partly or completely so that a controlled amount of turbulence due to the different angles of attack would prevent the energy from being absorbed excessively. Another method is the stall control mechanism which is the designing the aerodynamics of the blades in such a way that at high wind speeds, the turbulence is automatically increased and the excessive wind energy capture is automatically prevented. The latter method requires less maintenance of the wind turbines as the rotor blades do not have any loose details which may be damaged over the time [6].

2.2. Different types of the wind turbines

Wind turbines are either fixed-speed or variable-speed. Fixed-speed wind turbines rotate at a constant speed while variable-speed wind turbines rotate with a varying speed. In order to implement a fixed-speed wind turbine, a conventional induction generator may be used. Figure 2.2 demonstrates the general configuration of the required equipment in a fixed-speed wind turbine.

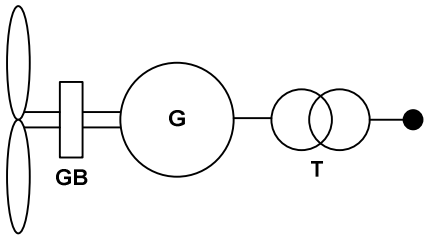

Figure 2.2 – A fixed-speed wind turbine system

Implementation of a variable-speed wind turbine may be done in either the full-power-conversion method or the partial-power-conversion method. In the full-power-conversion method, all the wind turbine power should be handled by the power electronics converter. The generators of such systems may be induction generators or synchronous generators. Figure 2.3 shows the general configuration of the required equipment in a full-power-conversion method.

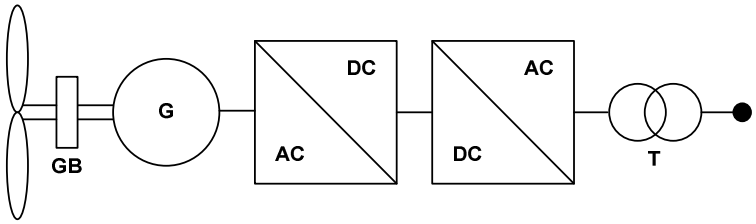

Figure 2.3 – A full-power-conversion system for a variable-speed wind turbine

Also, a partial-conversion-method may be employed in order to implement a variable-speed wind turbine system. In such systems, only a percentage of the wind turbine power is handled by the power electronics converter. This will reduce the power ratings of the needed power electronics equipment and also the losses. The generators of such systems are of the doubly-fed-induction-generator type. Figure 2.4 shows the general configuration of the required equipment in a partial-power-conversion method.

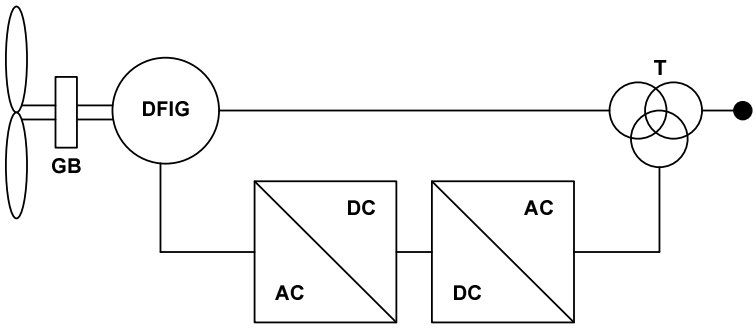

Figure 2.4 – A partial-power-conversion system for a variable-speed wind turbine

In the case of the full-power-conversion method, the voltage and frequency applied to the machine is manipulated by a controller so that the desired behaviour is obtained. In the case of the partial-power-conversion, a power electronics converter changes the frequency of the grid to a desired value and applies it to the rotor of the machine through the slip-rings. This means that the speed of the DFIG system may be controlled based on the DFIG system behaviour. One problem with this method is the required maintenance of the slip rings.

One of the main problems with the wind power is the fluctuating speed of the wind. As the converted wind power depends on the wind speed, the fluctuations in the wind speed will result in fluctuations in the converted power and the shaft torque. Lifetime expectancy of the wind turbine equipment, especially the gear-box component is decreased by such fluctuations. Fixed-speed wind turbines experience such fluctuations. One remedy to decrease the effects of the fluctuations of the torque is to use the variable-speed wind turbines. In variable-speed wind turbines, the speed is changed according to the input power. If the input power is increased, the speed of the turbine will be increased and vice-versa. As the power is a multiplication of the torque and the speed, this method will help to keep the torque in the system constant.

2.3. The wind energy conversion process

The wind contains energy. One could easily feel this fact through being pushed by it when there is a strong wind outdoors. The very same force can drive a turbine and force a generator to turn and in this way, electricity can be generated and the wind energy can be transported easily and efficiently and be used. The wind power may be captured and converted to mechanical power. The process is called the aerodynamic energy conversion and involves the air stream passing over the surface of the blades of a turbine and imposing a driving force on them. The converted power is proportional to the third power of the wind speed and is also proportional to the air density and the geometric area swept by the blades and also an aerodynamic conversion efficiency factor. The aerodynamic conversion efficiency factor depends on two variables: β and λ. β is the pitch angle of the blades and is decided by a controller, and λ is the tip speed ratio which is defined as the ratio between the linear speed of the tip of the blades and the wind speed.

$$\lambda = \frac{v_{tip}}{v_w} = \frac{R\omega}{v_w} \quad (2.1)$$

$$C_p = C_p(\beta, \lambda) \quad (2.2)$$

Figure 2.5 demonstrates the variable C_p as a function of the variables β and λ.

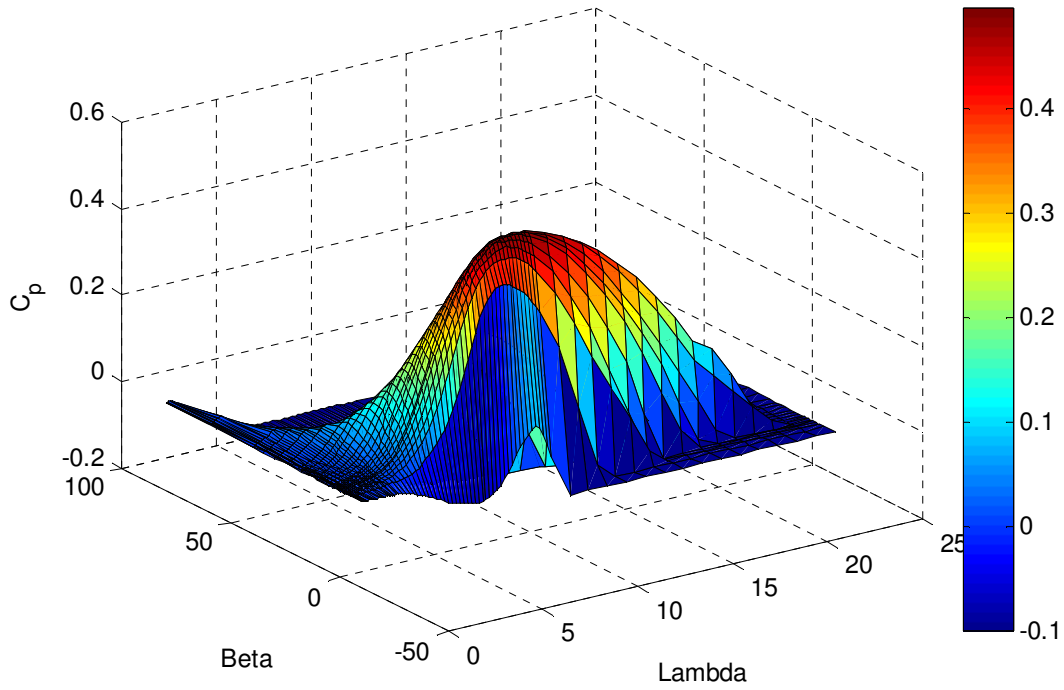

Figure 2.5 – Aerodynamic efficiency C_p as a function of β and λ

For any value of λ, a specific value of β exists that will lead to the highest value of C_p. Figure 2.6 demonstrates the maximum possible C_p for any value of λ.

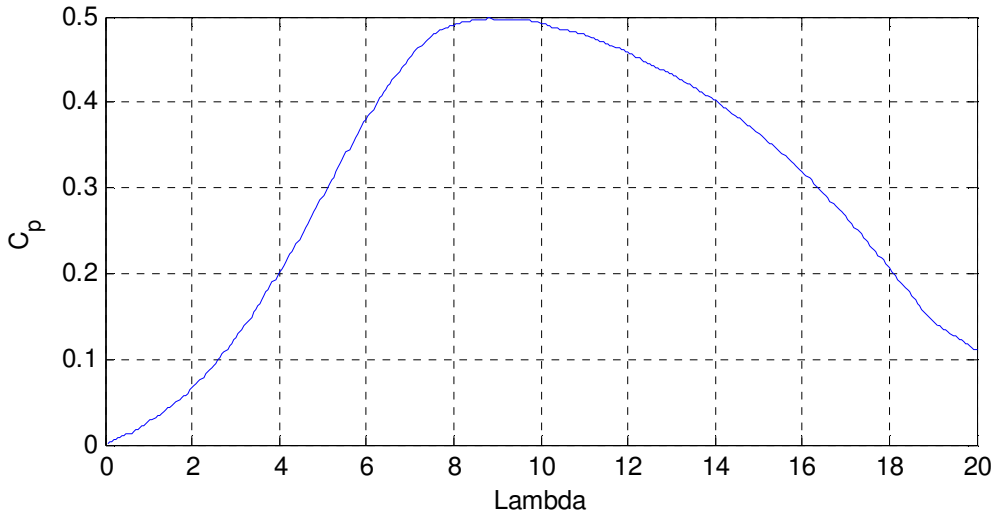

Figure 2.6 – Maximum possible C_p for different values of λ

The converted wind energy power may be calculated by the following formula [6]:

$$P = {}^{1}/_{2}\,\rho C_p(\beta,\lambda)Av_w{}^{3} \qquad (2.3)$$

Figure 2.7 demonstrates the output power of a wind turbine as a function of the incident wind speed.

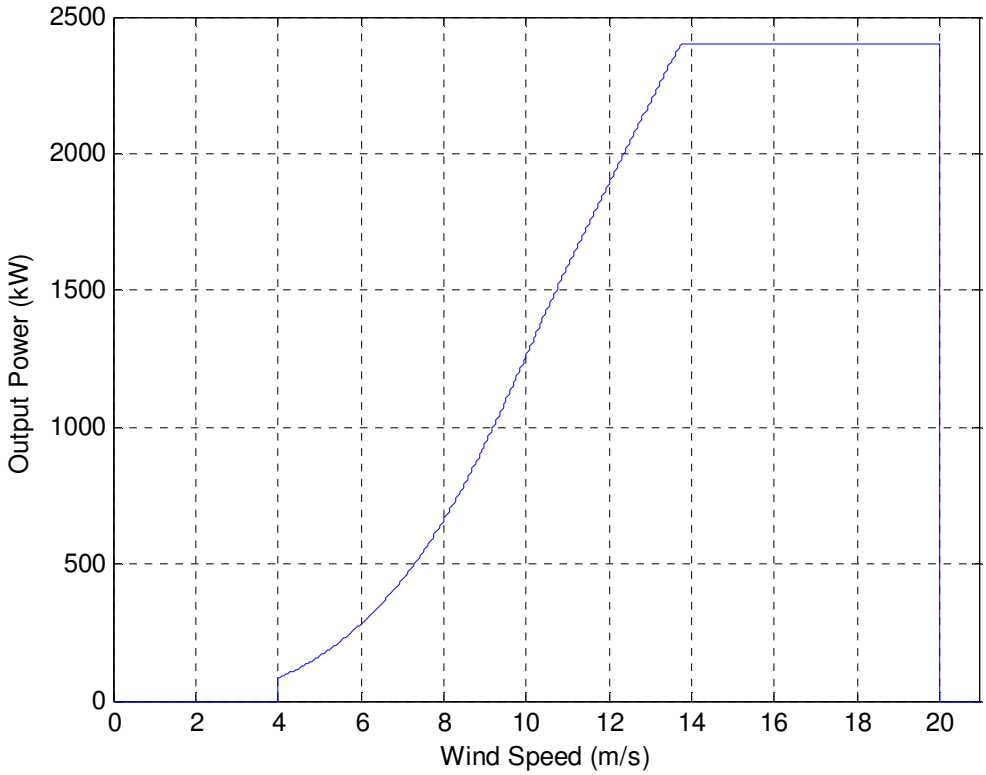

Figure 2.7 – Power curve of a wind turbine

It should be noted that there is a certain wind speed range for the wind turbine to work. Below the cut-in-speed and above the cut-out-speed, the wind turbine will be turned off automatically.

2.4. The characteristics of the wind speed

Due to the fact that the wind power depends directly on the wind speed value, a great deal of research has been devoted to mathematically modelling the wind speed. The wind speed probability distribution throughout a year is best described by Weibull distribution [6]:

$$f(v_w) = \frac{k}{c}\left(\frac{v_w}{c}\right)^{k-1} e^{-\left(\frac{v_w}{c}\right)^k} \qquad (2.4)$$

In which "k" is called the shape parameter and "c" is called the scale parameter. In the case of k = 2, the distribution is known as Rayleigh distribution and the mean wind speed in a year may be obtained through:

$$\overline{v_w} = c\sqrt{\pi}/2 \qquad (2.5)$$

The number of hours in a year that the wind speed is equal to a specific value may be calculated by multiplying the total number of hours in a year by the probability of the wind speed being equal to the that value:

$$N(\mathrm{v_w}) = \mathrm{T.f(v_w)} \quad (2.6)$$

$$In\ which: T = 365 \times 24 = 8760\ \mathrm{hr} \quad (2.7)$$

Figure 2.8 demonstrates a sample Weibull distribution of the number of hours in a year with specific wind speeds for an area with annual mean wind speed of 8 m/s.

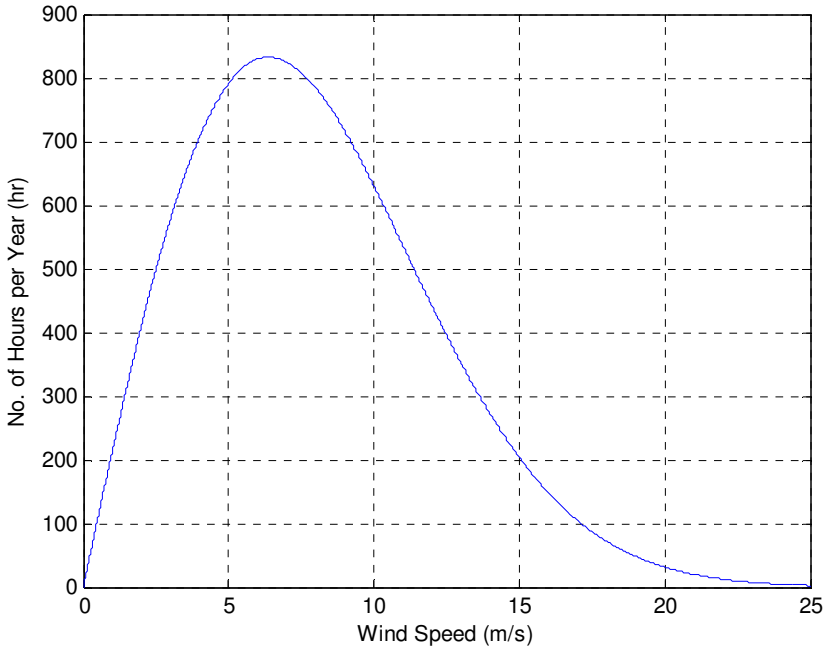

Figure 2.8 – No. of hours with a specific wind speed in an area with the mean wind speed 8 m/s

The annual amount of energy production for a wind farm or a single wind turbine may be calculated by the following formula:

$$E_{annual} = T.\int_{v_w=0}^{v_w=\infty} P(v_w).f(v_w)\,.dv_w \quad (2.8)$$

In which $P(v_w)$ is the output power of the wind farm or the wind turbine and $f(v_w)$ is the probability of the wind speed being equal to v_w.

Due to stochastic characteristics of the wind, the wind speed direction has a probabilistic nature. This means that a probability density function may describe the probability of the wind speed having a specific direction. The probability density function of the wind direction has a complex nature but through the long-term measurements, the general tendency of the wind direction may be obtained and used. The wind speed direction probability is usually described by the "Rose Diagram" which is basically a curve around an inner point representing a casual point in the area being studied. The points on the curve have the characteristic that their distance to central point is proportional to the probability of the wind blowing in the direction which is pointed by an arrow connecting the central point to the point on the curve. The Rose Diagram has also applications in airplane navigation and metrological studies. Figure 2.9 shows a sample Rose Diagram [7].

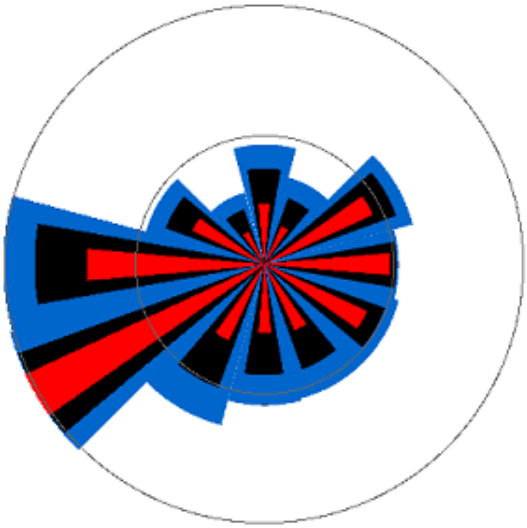

Figure 2.9 – A sample Rose Diagram

When the wind streams over the blades of a wind turbine, its speed decreases and becomes turbulent. Basically, the blades of the wind turbine turn the wind direction into a spiral form and the wind speed flux will be similar to some spirals after passing the turbine. The wake effects at "Horns Rev" and "Nysted" wind farms have been observed from the space by the satellites and have been confirmed [8]. Many efforts have been made in order to model the wake effects and its impact on the energy production in a wind farm. Especially, the wake effects at Horns Rev have been studied in detail. The studies show that there will be a substantial decrement in the average wind speed when the wind passes the first row of the turbines in a wind farm but the average speed at the turbines in the next rows will decrease in much less percentage than at the first row. An appropriate wake effect model for power system studies is a decrement in average wind speed at the distance x after the wind turbine [9, 10]:

$$v_w(x) = v_0.\left[1 - \left(\frac{R}{k_w x + R}\right)^2 (1 - \sqrt{1 - C_T})\right] \qquad (2.9)$$

In the above formula, C_T is called the thrust coefficient, k_w is called the wake effect coefficient, v_0 is the speed of the incident windfront and R is the radius of the wind turbine blades. C_T is dependent on the wind speed and may be found out from a lookup table which in turn may be calculated from the aerodynamic efficiency lookup table. In order to calculate the C_T lookup table from the aerodynamic efficiency lookup table, first of all, the actual power curve of the wind turbine (considering the cut-in-speed, cut-out-speed, maximum turbine speed and maximum power rating limits) should be calculated. In the next step, for each wind speed, an auxiliary variable called the "axial induction factor", "a" should be calculated so that $C_p(v_w) = 4a(1-a)^2$. As the analysis of this equation with the Maple software shows that the analytical solutions of this equation are complicated, the "fzero" function of MATLAB is recommended instead. When the variable "a" is become known, C_T could be calculated using the $C_T(v_w) = 4a(1-a)$ formula [11]. A sample C_T lookup table is shown in Figure 2.10.

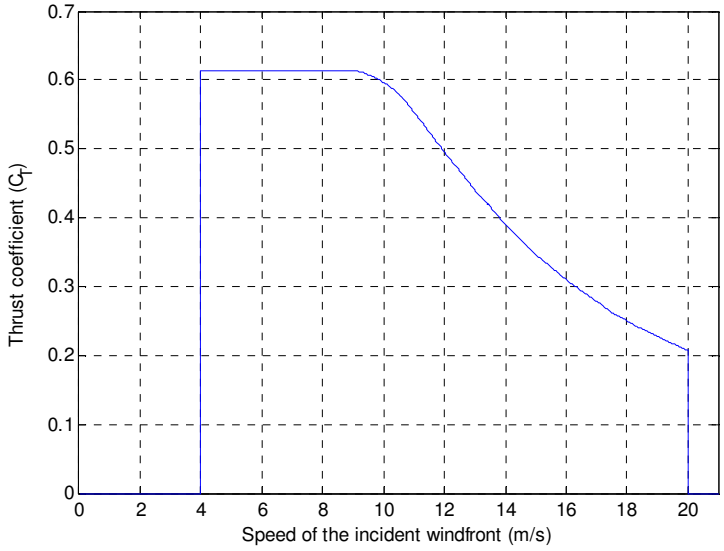

Figure 2.10 – Thrust coefficient as a function of the wind speed

The wake effect coefficient is usually a number between $k_w = 0.05$ and $k_w = 0.11$ and depends on the surface on which the wind blows. Typical values of $k_w = 0.05$ and $k_w = 0.08$ are recommended for offshore and onshore wind farm studies [12]. Considering a typical value of $k_w = 0.05$ for offshore applications, Figure 2.11 demonstrates the coefficients of the wind speed due to the wake effects the distance x = 0.5 km after a wind turbine with a blades radius of R = 37 m.

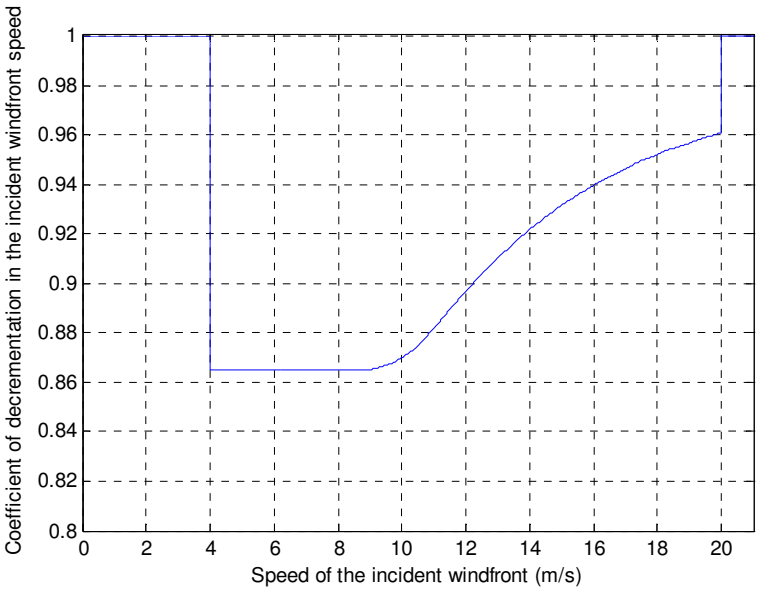

Figure 2.11 – Reduction coefficient of the wind speed due to the wake effects

3. Modelling the wind turbines

Modelling a wind turbine plays a key role in the process of engineering a wind turbine and all related parts of the power system. In order to study its operation, a suitable model is necessary. Figure 3.1 shows different parts which need to be modelled in order to study the relation between the input wind energy and the converted electric energy.

Figure 3.1 – Different interfaces in the wind energy conversion process

In this thesis work, it is assumed that the generator used in the wind turbine is an ordinary induction machine. The dynamic model of the induction machine is used but in addition, the non-stiffness of the blades of a wind turbine has been modelled as a double-mass interface and its effect has been taken into account. Moreover, there is a gear-box present in the system and it is placed inside the double-mass interface, so, the operation of the system will also be influenced by the gear-box and the natural frequencies of the system depend on the gear-box ratio. The mechanical energy absorbed by the blades of the wind turbine is determined by (2.3).

3.1. Modelling the induction machine

The well-known dynamic model of the induction machine may be used to study its transient operation in a wind turbine.

$$R = \begin{pmatrix} R_s & 0 & 0 & 0 \\ 0 & R_s & 0 & 0 \\ 0 & \omega_r L_m & R_r & \omega_r L_r \\ -\omega_r L_m & 0 & -\omega_r L_r & R_r \end{pmatrix} \tag{3.1}$$

$$L = \begin{pmatrix} L_s & 0 & L_m & 0 \\ 0 & L_s & 0 & L_m \\ L_m & 0 & L_r & 0 \\ 0 & L_m & 0 & L_r \end{pmatrix} \tag{3.2}$$

$$\underline{v} = L\frac{d\underline{i}}{dt} + R\underline{i} \Rightarrow \frac{d\underline{i}}{dt} = -L^{-1}R\underline{i} + L^{-1}\underline{v} \tag{3.3}$$

$$\emptyset_s = (L_m + L_s)i_s + L_m i_r \tag{3.4}$$

$$T_e = \frac{3n_p}{2}\left(\emptyset_{s\alpha} i_{s\beta} - \emptyset_{s\beta} i_{s\alpha}\right) \tag{3.5}$$

$$\frac{J}{n_p}\frac{d\omega_r}{dt} = T_e - T_m \tag{3.6}$$

The steady-state model of the induction machine may be used to study its steady-state operation. Figure 3.2 demonstrates the steady-state model of the induction machine.

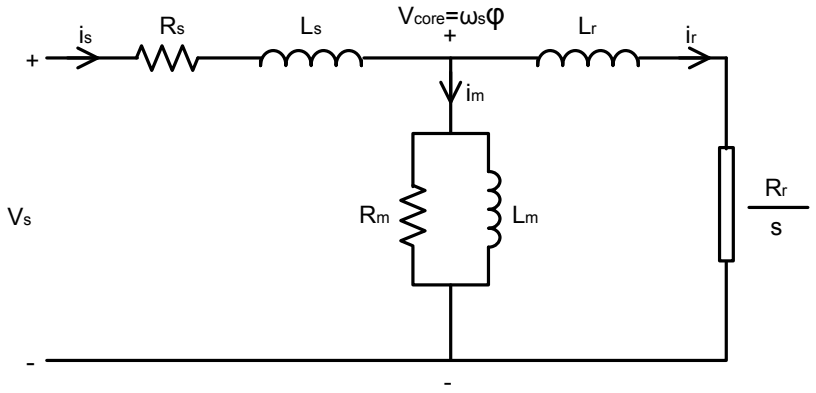

Figure 3.2 – Steady-state model of the induction machine

Based on the steady-state model of the induction machine, the converted mechanical power and torque may be calculated through the following formulas:

$$P_m = 3\frac{1-s}{s}R_r|i_r|^2 \quad (3.7)$$

$$T_m = \frac{P_m}{\Omega_m} = \frac{n_p P_m}{\omega_m} \quad (3.8)$$

The stator and copper losses can also be calculated through:

$$P_s = 3R_s|i_s|^2 \quad (3.9)$$

$$P_r = 3R_r|i_r|^2 \quad (3.10)$$

More detailed analysis of the stator and rotor losses will come in the next chapter. The iron losses in the induction machines mainly depend on two components: The hysteresis losses and the eddy-currents losses. Dependency of these two components of the losses on the machine flux and the frequency is rather complicated in nature but may be simplified in two formulas as below.

$$P_h = k_h f \varphi^n \qquad (1.5 < n < 2.5) \quad (3.11)$$

$$P_e = k_e f^2 \varphi^2 \quad (3.12)$$

In basic simulations, "n" may be approximated to be equal to 2. The iron losses may be approximated through the addition of the two latter formulas:

$$P_{Fe} = P_h + P_e = k_h f \varphi^2 + k_e f^2 \varphi^2 \quad (3.13)$$

The iron losses are usually represented in the machine model through a resistance in parallel with the rotor circuit. In order to derive a formula for R_m, the fact that the flux in the machine depends on the voltage and the frequency should be considered.

$$\varphi = \frac{V_{core}}{2\pi f} \Rightarrow P_{Fe} = 3\frac{V_{core}^2}{R_m} = 3\frac{4\pi^2 f^2 \varphi^2}{R_m} \quad (3.14)$$

The energy dissipation in the resistance R_m should be equal to the iron losses.

$$\frac{12\pi^2 f^2 \varphi^2}{R_m} = k_h f \varphi^2 + k_e f^2 \varphi^2 \quad (3.15)$$

Hence:

$$R_m \cong \frac{12\pi^2 f}{k_h + k_e f} \quad (3.16)$$

In this thesis work, as the ratio between the hysterisys losses and the eddy-current losses of the core of the wind turbine generator used in the simulations were not specified in the datasheet of the wind turbine generator, the frequency-dependency of R_m was not taken into account but in the derivations of the formulas and the methods, the frequency-dependent nature of R_m was considered and the results are general.

3.2. Modelling the non-stiff shaft and the gear-box

The natural consequence of a non-stiff shaft in a wind turbine may be mechanically modelled as a spring which exists between the blades hub and the generator shaft. The damping characteristic which results from the non-stiffness is required in order to prevent the system from getting damaged by the fluctuating torques on the shaft. It has also certain effects in the voltage stability studies [13]. P_{wind} is determined by (2.3). In addition, a gear-box is also present in the wind turbine system that enables the high-speed induction generator to be driven by the low-speed blades. When the gear-box is present in the system, it plays a key role in the natural frequencies of the system as its ratio will appear in the state-space matrices. The gear-box may be placed in two positions. It can be either between the blades hub and the spring or between the generator shaft and the spring. In this thesis work, the gear-box is assumed to be between the spring and the generator shaft. Figure 3.3 demonstrates a double-mass interface with a gear-box on the low-speed side representing the mechanical model of the non-stiff shaft and the gear-box of the wind turbine.

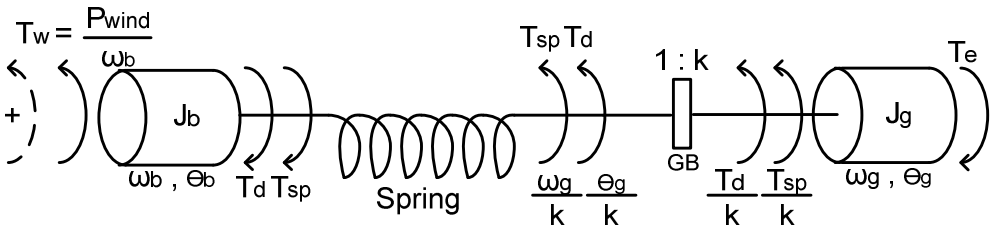

Figure 3.3 – Equivalent mechanical model of the shaft and the gear-box of the wind turbine

When two inertias are connected to each other through a spring, they interact with each other through the torque components transferred by the spring. The force the spring transfers between the two inertias depends on the angle and speed difference between them.

$$T_{sp} = k_{sp}.\left(\theta_b - {}^{\theta_g}/_{k}\right) \tag{3.17}$$

$$T_d = k_d.(\omega_b - {}^{\omega_g}/_{k}) \tag{3.18}$$

In order to model the system, Newton's second law should be applied to both the inertias:

$$J_b \frac{d\omega_b}{dt} = T_w - T_{sp} - T_d \tag{3.19}$$

$$J_g \frac{d\omega_g}{dt} = {}^{T_{sp}}/_{k} + {}^{T_d}/_{k} - T_e \tag{3.20}$$

Also, based on the definitions:

$$\omega_b = \frac{d\theta_b}{dt} \tag{3.21}$$

$$\omega_g = \frac{d\theta_g}{dt} \tag{3.22}$$

Considering above-mentioned equations, state-space model of the system may be derived with speeds and angles of two inertias as state variables and input and output torques as input variables.

$$\begin{pmatrix} \frac{d\omega_b}{dt} \\ \frac{d\omega_g}{dt} \\ \frac{d\theta_b}{dt} \\ \frac{d\theta_g}{dt} \end{pmatrix} = \begin{pmatrix} -\frac{k_d}{J_t} & \frac{k_d}{kJ_t} & -\frac{k_{sp}}{J_t} & \frac{k_{sp}}{kJ_t} \\ \frac{k_d}{kJ_g} & -\frac{k_d}{k^2J_g} & \frac{k_{sp}}{kJ_g} & -\frac{k_{sp}}{k^2J_g} \\ 1 & 0 & 0 & 0 \\ 0 & 1 & 0 & 0 \end{pmatrix} . \begin{pmatrix} \omega_b \\ \omega_g \\ \theta_b \\ \theta_g \end{pmatrix} + \begin{pmatrix} \frac{1}{J_b} & 0 \\ 0 & -\frac{1}{J_g} \\ 0 & 0 \\ 0 & 0 \end{pmatrix} \begin{pmatrix} T_w \\ T_e \end{pmatrix} \tag{3.23}$$

In order to obtain the natural frequencies of the system, the following equation should be solved:

$$A = \begin{pmatrix} -\frac{k_d}{J_t} & \frac{k_d}{kJ_t} & -\frac{k_{sp}}{J_t} & \frac{k_{sp}}{kJ_t} \\ \frac{k_d}{kJ_g} & -\frac{k_d}{k^2J_g} & \frac{k_{sp}}{kJ_g} & -\frac{k_{sp}}{k^2J_g} \\ 1 & 0 & 0 & 0 \\ 0 & 1 & 0 & 0 \end{pmatrix} \Rightarrow \det(sI - A) = 0 \tag{3.24}$$

The solution of the equation will be:

$$s = -\frac{1}{2}\frac{J_t k_d + J_g k_d k^2 \pm \sqrt{-4k_{sp}{J_g}^2 J_t k^4 + {J_g}^2 {k_d}^2 k^4 - 4k_{sp} J_g {J_t}^2 k^2 + 2J_g J_t {k_d}^2 k^2 + {J_t}^2 {k_d}^2}}{J_g J_t k^2} \tag{3.25}$$

A sample frequency response of a non-stiff shaft with a gear-box is shown in Figure 3.4.

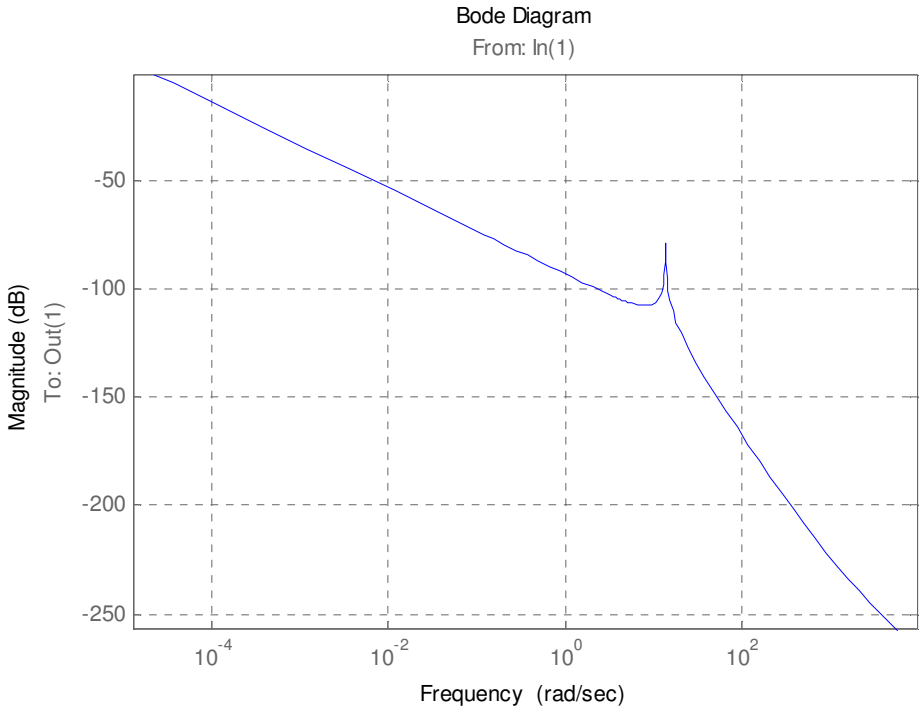

Figure 3.4 – Frequency response of a double-mass interface with a gear-box

3.3. Integration of the induction machine model with the non-stiff shaft and the gear-box model

The existence of the double-mass interface and the gear-box influence the behaviour of the system as they change the state-space model. Electrical equations which have been derived actually do not change. The electric torque developed on the shaft of the machine will have to be applied to the double-mass interface and along with the torque from the wind, the response of the speeds of both the blades and the shaft will be determined. The speed response of the generator shaft speed will influence the electrical equations model as they are non-linear time-varying and functions of the shaft electrical speed. Also, the speed response of the blades will influence the wind energy conversion process as the tip speed ratio and consequently the aerodynamic efficiency depends on it.

3.4. Modelling the transformer of a wind turbine generator and the connection cable

In most of the wind turbine system designs, there is a transformer included in order to step up the voltage of the generator so that the transmission losses are decreased in the offshore grid. In order to analyze the behaviour of the wind turbine transformer, the equivalent circuit model of a power transformer may be used. Figure 3.5 demonstrates the equivalent circuit of a power transformer.

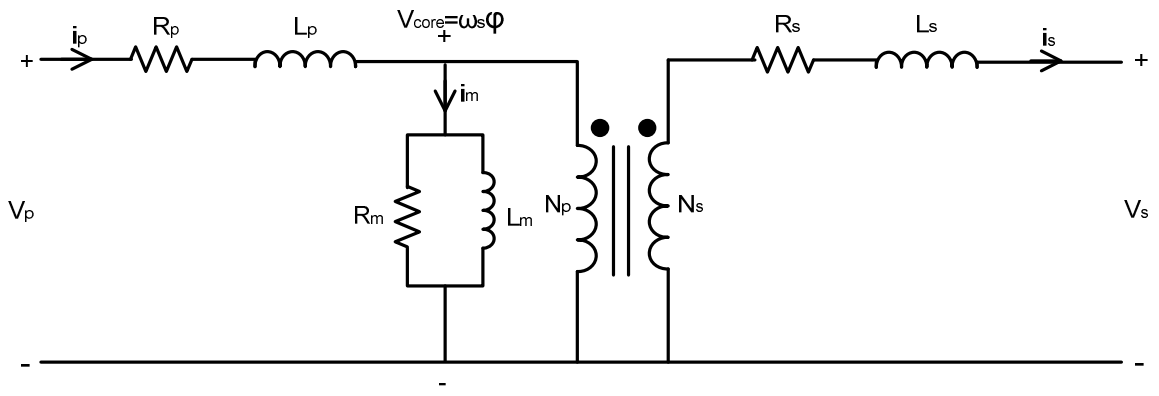

Figure 3.5 – Equivalent circuit of a transformer

It is possible to simplify the mentioned equivalent circuit through moving all of the components to only one side of the ideal transformer using the corresponding formulas. Figure 3.6 shows the simplified equivalent circuit of a power transformer.

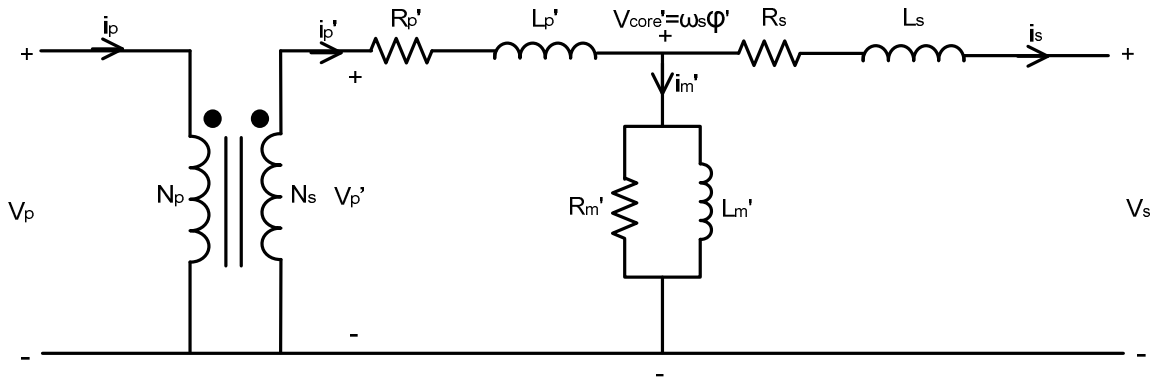

Figure 3.6 – Simplified equivalent circuit of a transformer

The losses in a power transformer consist of two components: The copper losses and the core losses. The copper losses consist of two components: The copper losses in the primary circuit and the copper losses in the secondary circuit.

$$P_p = 3R_p|i_p|^2 = 3R_p'|i_p'|^2 \quad (3.26)$$

$$P_s = 3R_s|i_s|^2 = 3R_s'|i_s'|^2 \quad (3.27)$$

The core losses in a transformer are similar to the ones in a generator. Therefore, they may be summarized in a similar manner.

$$P_{Fe} = P_h + P_e = k_h f\varphi^2 + k_e f^2\varphi^2 = 3\frac{V_{core}^2}{R_m} \quad (3.28)$$

$$R_m \cong \frac{12\pi^2 f}{k_h + k_e f} \quad (3.29)$$

In the most of the power system analysis, it is possible to simplify the equivalent circuit of the transformer by moving all of the series impedances of the transformer to only one side of the

subcircuit representing the core. This will make it easier to identify the transformers by reducing the number of variables required to identify the transformer. Figure 3.7 demonstrates the approximate model of a transformer.

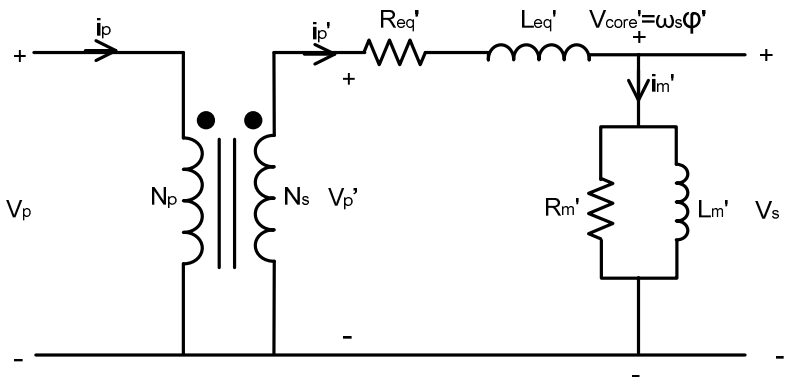

Figure 3.7 – Approximate equivalent circuit of a transformer

In which:

$$R'_{eq} = R'_p + R_s \tag{3.30}$$

$$L'_{eq} = L'_p + L_s \tag{3.31}$$

There are also power cables required to connect the wind turbines in an offshore grid. A simple representation of the connection cables is demonstrated in Figure 3.8.

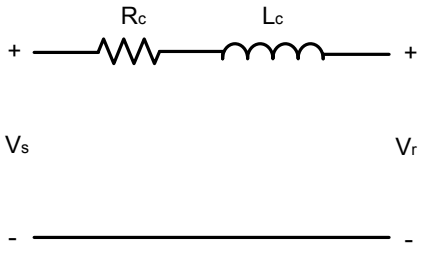

Figure 3.8 – Equivalent circuit of a connection cable

The losses in a connection cable originate from the resistive part of the equivalent circuit.

$$P_c = 3R_c|i_c|^2 \tag{3.32}$$

It is possible to consider the effect of the connection cable in the primary side of the transformer by adding the parameters of the connection cable to the corresponding parameters of the primary side of the transformer. In this thesis work, in the main part of the derivations of the formulas for the reference voltage and frequency of the offshore grid and the control strategy schematics, the transformer and the cable is not considered but in the end of that part, the guidelines for inclusion of

the transformer and the cables are provided. Moreover, an approximate method for inclusion of the transformer core in the loss minimization process is provided.

4. Proposals for efficiency improvements in the offshore grid

4.1. The case of a single wind turbine as a base for the wind farm case

In order to develop the formulas and look-up tables for the case of a wind farm, the simpler case of a single wind turbine is analyzed first and the methods for the efficiency improvements are suggested. Figure 4.1 demonstrates the control strategy of a single wind turbine which is to be studied.

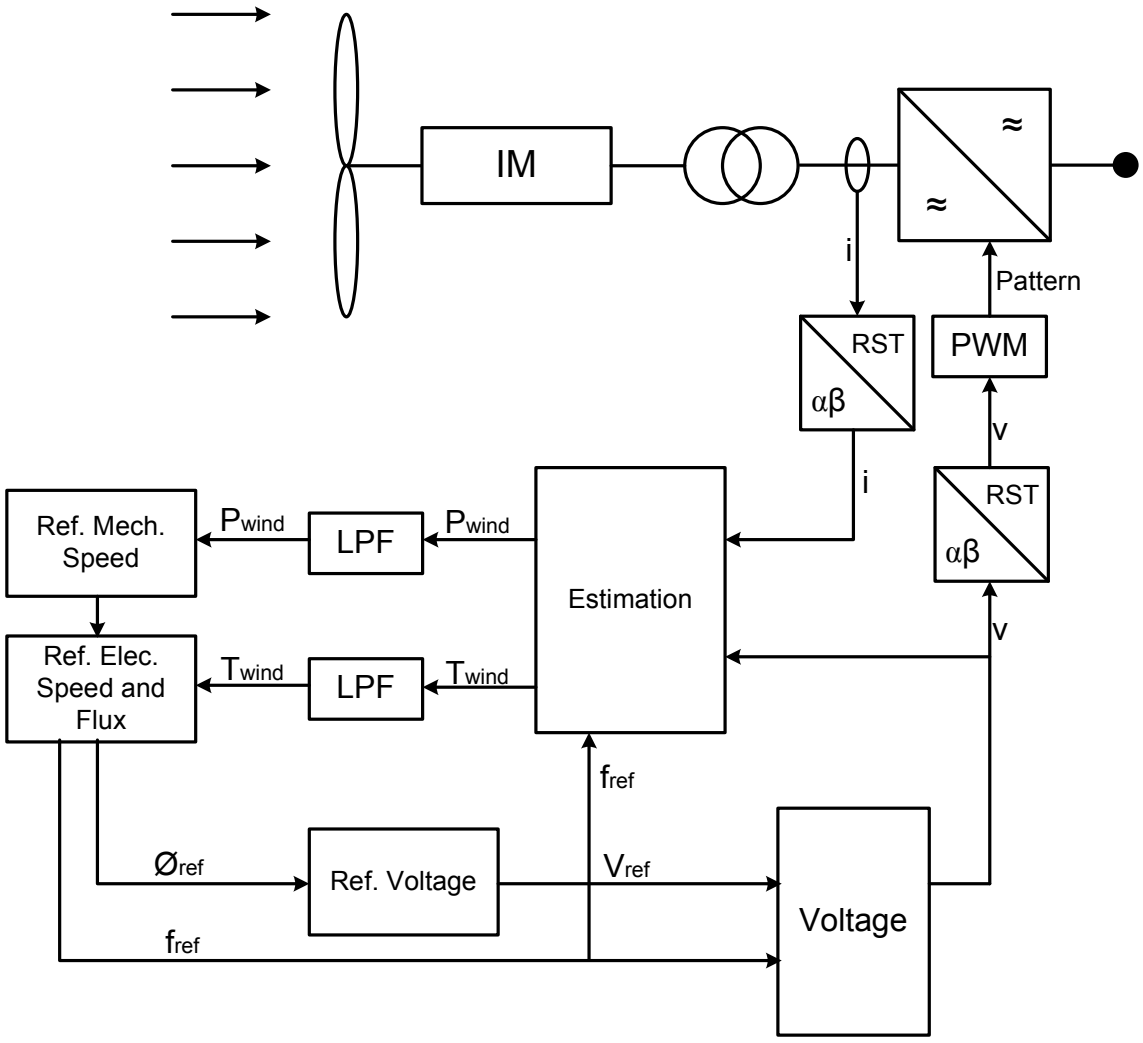

Figure 4.1 – The overview of the strategy for a single wind turbine

The machine flux is a very important variable in the machine since the machine losses depend on it. Figure 3.2 demonstrates the equivalent steady-state model of the induction machine. The rotor current is approximately proportional to the ratio of the shaft torque and the reference flux. Hence, for a specific torque, the rotor current decreases if the flux is increased and the rotor current increases if the flux is decreased. As the rotor current passes through the stator and the rotor resistances, the power dissipated in the rotor resistance is inversely related to the square of the flux. The magnetizing current in an induction machine is also affected by the machine flux. The higher the flux, the higher the magnetizing current. Maintaining a strong magnetic field inside the machine would lead to a high amount of iron losses in the core which is approximately proportional to the square of the flux. Hence,

some loss components of the machine increase with increasing the flux while some others decrease with increasing the flux. A certain optimum flux may be calculated so that the losses in machine will be minimized. The rotor current is determined by the torque on the shaft and flux in the machine.

$$|i_r| = \frac{|V_{core}|}{|Z_r|} = \frac{|V_{core}|}{\sqrt{\left(\frac{R_r}{s}\right)^2 + X_r^2}} = \frac{\omega_s \varphi}{\sqrt{\left(\frac{\omega_s R_r}{\omega_s - \omega_m}\right)^2 + (\omega_s L_r)^2}} = \frac{\varphi}{\sqrt{(A R_r)^2 + (L_r)^2}} \quad (4.1)$$

"A" is an auxiliary variable defined as:

$$A = \frac{1}{\omega_s - \omega_m} \quad (4.2)$$

The mechanical power exchanged with the shaft may be calculated.

$$P_m = 3\frac{1-s}{s} R_r |i_r|^2 = 3\frac{\omega_m}{\omega_s - \omega_m} R_r |i_r|^2 \quad (4.3)$$

The torque developed on the shaft may be calculated.

$$T_m = \frac{n_p P_m}{\omega_m} = 3n_p \frac{1-s}{\omega_m s} R_r |i_r|^2 = 3n_p \frac{1}{\omega_s - \omega_m} R_r |i_r|^2 = \frac{3n_p A R_r \varphi^2}{{R_r}^2 A^2 + {L_r}^2} \quad (4.4)$$

$$T_m = {}^3\!/_2 \frac{n_p A R_r \hat{\varphi}^2}{{R_r}^2 A^2 + {L_r}^2} \quad (4.5)$$

It should be noted that for simulation purposes, $\hat{\varphi}$ (the peak value) is used in the latter equation instead of φ (the RMS value). Due to this reason, a coefficient of ${}^1\!/_2$ is required. In order to simplify the equation, it is possible to take advantage of an auxiliary variable "k".

$$k = {}^3\!/_2 n_p R_r \hat{\varphi}^2 \,,\; A = \frac{1}{\omega_s - \omega_m} \quad (4.6)$$

$$T_m = \frac{kA}{R_r^2 A^2 + L_r^2} \Rightarrow (T_m R_r^2) A^2 - kA + T_m L_r^2 = 0 \quad (4.7)$$

This is a quadratic equation for which the solution is readily available.

$$\Delta = k^2 - 4{T_m}^2 R_r^2 L_r^2 \quad (4.8)$$

$$A = \frac{k + \sqrt{\Delta}}{2 T_m R_r^2} \quad (4.9)$$

All the variables in the machine may be calculated based on "A". The rotor current is already calculated. The stator current may also be calculated. ($X_m \ll R_m$)

$$|i_s| = \frac{|V_{core}|}{\left|\left(\frac{R_r}{s} + jX_r\right) \| jX_m \| R_m\right|} = \frac{\varphi}{\sqrt{(A R_r)^2 + (L_r)^2}} . \frac{\sqrt{(A R_r)^2 + (L_r + L_m)^2}}{L_m} \quad (4.10)$$

The stator and rotor losses may be calculated respectively.

$$P_s = 3R_s|i_s|^2 = {}^3\!/_2\, R_s \frac{\hat{\varphi}^2}{(A R_r)^2+(L_r)^2} \frac{(A R_r)^2+(L_r+L_m)^2}{{L_m}^2} \quad (4.11)$$

$$P_r = 3R_r|i_r|^2 = {}^3\!/_2\, R_r \frac{\hat{\varphi}^2}{(A R_r)^2+(L_r)^2} \quad (4.12)$$

Moreover, the iron losses may be included also.

$$P_{Fe} = P_h + P_e = k_h f\varphi^2 + k_e f^2\varphi^2 \quad (4.13)$$

Other losses in the machine and even other used equipment may also be included and the method will seamlessly work. In the case of inclusion of the losses of the employed transformers or converters, numerical methods may be used.

$$P_{loss} = P_s + P_r + P_{Fe} + P_{etc} \quad (4.14)$$

The losses function may be differentiated and equated to zero in order to obtain the optimal flux for the machine operation. An analytical approach for minimizing (4.14) may lead to equations that may not be possible to be solved analytically, in such cases, numerical methods may be used instead. From a practical point of view, the "fzero" function in MATLAB or the "solve" function in Maple or a custom FORTRAN function for PSCAD/EMTDC which will not be very difficult to implement or even a look-up table in real situations may be used. In MATLAB simulations, the "min" and "fminsearch" functions may also be used. As a suggestion, the half interval method (binary search) may be a good solution for getting close to the minimum loss point through solving the equation of the derivative of the loss function. On the other hand, through an approximate method which will be evaluated later, a simpler solution may be obtained. In order to derive the approximate method, the following equations should be considered. Figure 3.2 demonstrates the equivalent steady-state circuit of an induction machine.

$$\begin{cases} |i_r| \approx \frac{P_m}{3V_{core}} \\ |i_s|^2 \approx \frac{{P_m}^2}{9{V_{core}}^2} + \frac{{V_{core}}^2}{{X_m}^2} \end{cases} \quad (4.15)$$

$$\begin{cases} P_{Fe} = 3\frac{{V_{core}}^2}{R_{Fe}} \\ P_{Cu} = 3R_s|i_s|^2 + 3R_r|i_r|^2 \end{cases} \quad (4.16)$$

$$P_{loss} = P_{Fe} + P_{Cu} = 3\frac{{V_{core}}^2}{R_{Fe}} + 3(R_s + R_r)\frac{{P_m}^2}{9{V_{core}}^2} + 3R_s\frac{{V_{core}}^2}{{X_m}^2} \quad (4.17)$$

$$P_{loss} = \left(\frac{3}{R_{Fe}} + \frac{3R_s}{{X_m}^2}\right){V_{core}}^2 + \frac{(R_s+R_r){P_m}^2}{3}\frac{1}{{V_{core}}^2} \quad (4.18)$$

$$\begin{cases} A = \frac{3}{R_{Fe}} + \frac{3R_s}{{X_m}^2} \\ B = \frac{(R_s+R_r){P_m}^2}{3} \end{cases} \quad (4.19)$$

$$P_{loss} = A{V_{core}}^2 + B{V_{core}}^{-2} \Rightarrow \frac{dP_{loss}}{dV_{core}} = 2AV_{core} - 2B{V_{core}}^{-3} = 0 \quad (4.20)$$

$$V_{core} = \sqrt[4]{\frac{B}{A}} = \sqrt[4]{\frac{(R_s+R_r){P_m}^2}{3(\frac{3}{R_{Fe}}+\frac{3R_s}{{X_m}^2})}} = \sqrt[4]{\frac{R_{Fe}{X_m}^2(R_s+R_r){P_m}^2}{9({X_m}^2+R_{Fe}R_s)}} \quad (4.21)$$

Induction machines are based on the principle of the induction of current into the rotor circuit due to the speed difference of the stator flux and the rotor circuit. As the torque on the shaft increases, the speed difference between the stator and the rotor increases and also the frequency of the current in the rotor circuit increases. Due to this fact, the induction machines run at a speed near the electrical frequency of the stator electrical voltage but slightly higher or lower depending on whether they are operated as generators or motors. As the dynamic equations of the induction machines may be simplified into a certain steady-state model for steady-state studies, for applications like the one here where transient response is not of great interest, a controller may adjust the stator frequency based on the derived model so that the motor operates at the desired speed. In this method, the controller calculates a specific frequency which if applied to the stator, would result in the reference rotor mechanical speed. In order to find this specific frequency, the converted power in the machine and the converted torque on the shaft may be estimated and equated to the relevant values and after solving the equations, this certain electrical frequency may be obtained. As the wind speed changes, λ changes and C_P value will consequently change. A certain λ_{max} exists that corresponds to $C_{P,max}$, the maximum aerodynamic efficiency. In order to keep the efficiency at the maximum point, there should be a controller installed in the system which should constantly set the rotational speed reference according to the wind speed. But as the wind speed may not be measured directly, another approach should be taken. The output power from the turbine may be measured and the speed can be tuned according to the measured power, so that the efficiency gets maximized.

$$P = {}^1\!/_2\,\rho C_p A {v_w}^3 \quad (4.22)$$

$$\lambda_{opt} = \frac{R\omega}{v_w} \Rightarrow v_w = \frac{R\omega}{\lambda_{opt}} \quad (4.23)$$

$$P = {}^1\!/_2\,\rho C_{p,max} A \frac{R^3 {\omega_{ref}}^3}{{\lambda_{opt}}^3} \Rightarrow \quad (4.24)$$

$$\omega_{ref} = \frac{\lambda_{opt}}{R}\sqrt[3]{\frac{2}{\rho A C_{p,max}}}\sqrt[3]{P} \quad (4.25)$$

Hence, in order to maximize the conversion process efficiency, the output power should be continuously measured and be used to determine the reference speed of the turbine. To derive the reference electrical frequency formula, first of all, the shaft torque on the machine should be calculated. The core voltage should be adjusted according to the stator frequency so that the desired value for the flux magnitude is obtained.

$$V_{core} = \varphi_{ref}.\omega_s \quad (4.26)$$

The rotor current may be calculated according to the core voltage and the slip.

$$I_r = \frac{V_{core}}{{R_r}/{s}+jX_r} \Rightarrow |I_r|^2 = \frac{{\varphi_{ref}}^2.{\omega_s}^2}{\left({R_r}/{s}\right)^2+{X_r}^2} \quad (4.27)$$

The mechanical power on the shaft may be calculated according to the rotor current magnitude.

$$P_m = {}^3\!/_2 \frac{1-s}{s} R_r \left|\hat{I}_r\right|^2 \Rightarrow P_m = {}^3\!/_2 \frac{\omega_m}{\omega_s-\omega_m} R_r \frac{\hat{\varphi}_{ref}{}^2}{\left(\frac{R_r}{\omega_s-\omega_m}\right)^2+L_r^2} \quad (4.28)$$

So, it is possible to calculate the torque on the shaft.

$$\Rightarrow T_m = {}^{n_p P_m}\!/_{\omega_r} = {}^3\!/_2 \frac{n_p}{\omega_s-\omega_m} R_r \frac{\hat{\varphi}_{ref}{}^2}{\left(\frac{R_r}{\omega_s-\omega_m}\right)^2+L_r^2} \quad (4.29)$$

The latter equation may be reversely used to calculate a certain value of ω_s based on a T_m and ω_m which would result in the machine operating in the state desired by the controller. As ω_s and ω_m are two variables with close numerical values, solving the equation in a simulation software like MATLAB/Simulink or PSCAD/EMTDC would not achieve the desired precision and would result in the divergence of the results. The point is that in a digital controller or a simulation software $A = \frac{1}{\omega_s-\omega_m}$ should be considered as the unknown variable not the $(\omega_s - \omega_m)$ itself due to the round-off errors.

Therefore:

$$k = {}^3\!/_2 R_r n_p \hat{\varphi}_{ref}{}^2 \,,\; A = \frac{1}{\omega_s-\omega_m} \quad (4.30)$$

$$T_m = \frac{kA}{R_r^2A^2+L_r^2} \Rightarrow (T_m R_r^2)A^2 - kA + T_m L_r^2 = 0 \quad (4.31)$$

This is a quadratic equation for which the solution is readily available.

$$\Delta = k^2 - 4T_m{}^2 R_r^2 L_r^2 \quad (4.32)$$

$$A = \frac{k+\sqrt{\Delta}}{2T_m R_r^2} \quad (4.33)$$

"A" can be either positive or negative which corresponds to the motor or generator operating modes. In this work, the negative A is used as the induction machines are operated in the wind turbines in the generator mode. Hence:

$$\omega_s - \omega_m = \frac{1}{A} \Rightarrow \omega_{s,ref} = \omega_m + \frac{1}{A} \quad (4.34)$$

It should be noted that in the generator operation mode, "A" is usually a negative number, so, in order to have a specific speed for the machine shaft, an electrical speed with a frequency which is slightly lower than the desired speed should be applied. $\omega_{s,ref}$ will be the angular frequency of the offshore grid. Based on the induction machine equations, the torque developed on the shaft is proportional to the multiplication of the rotor current and the flux magnitude. As the torque on the shaft changes, the rotor current varies and this affects the stator current and due to the voltage drop on the stator impedance, the voltage at the core point and consequently the machine flux changes. In order to

obtain a desired flux magnitude, the voltage magnitude applied to the terminals of the machine should be manipulated so that the effect of the varying voltage drop on the stator impedance gets cancelled.

$$Z_{eq} = (jX_m) \parallel \left({R_r}/{s} + jX_r\right) = \frac{-X_m X_r + j\frac{X_m R_r}{s}}{{R_r}/{s} + j(X_r + X_m)} \tag{4.35}$$

Hence, the stator current may be calculated according to the core voltage.

$$I_s = \frac{V_{core}}{Z_{eq}} = \frac{(V_{core})({R_r}/{s} + j(X_r + X_m))}{-X_m X_r + j\frac{X_m R_r}{s}} \tag{4.36}$$

The stator voltage which will lead to this core voltage may now be calculated based on the known values.

$$V_s = (R_s + jX_s)I_s + V_{core} = (R_s + jX_s)\frac{(V_{core})({R_r}/{s} + j(X_r + X_m))}{-X_m X_r + j\frac{X_m R_r}{s}} + V_{core} \tag{4.37}$$

The latter equation should be simplified.

$$V_s = V_{core} \cdot \left(\frac{(-X_m X_r + \frac{R_s R_r}{s} - X_s(X_r + X_m)) + j(\frac{X_m R_r}{s} + R_s(X_r + X_m) + \frac{R_r X_s}{s})}{-X_m X_r + j\frac{X_m R_r}{s}}\right) \tag{4.38}$$

Therefore:

$$|V_s| = V_{core,ref} \cdot \left(\frac{(-X_m X_r + \frac{R_s R_r}{s} - X_s(X_r + X_m))^2 + (\frac{X_m R_r}{s} + R_s(X_r + X_m) + \frac{R_r X_s}{s})^2}{(-X_m X_r)^2 + (\frac{X_m R_r}{s})^2}\right) \tag{4.39}$$

In which:

$$V_{core,ref} = \varphi_{ref} \cdot \omega_{s,ref} \tag{4.40}$$

It should also be noted that whenever the reference frequency is changed, the impedances should be recalculated by the controller based on the new reference frequency. In an offshore wind farm whose converted energy is transported via an HVDC link, there will be no speed sensors available. As was described earlier, the concept of slip compensation is based on the calculation of the slip and then calculation of the stator voltage frequency from the rotor speed. Hence, in this method the rotor speed needs to be known while it is not directly available. During the steady-state operation, the steady-state model of the induction machine describes its behaviour and accordingly it may be used to estimate the machine slip. First of all, if the voltages and currents at the terminals of the machine are transferred to the αβ-domain, an equivalent impedance may be defined at the terminals of the machine resulting from the division of voltage and current at that point. The mentioned impedance may be used to estimate the slip in the machine.

$$Z_{eq} = (R_s + jX_s) + jX_m \parallel \left({R_r}/{s} + jX_r\right) \Rightarrow \tag{4.41}$$

$$\frac{1}{R_{eq}+jX_{eq}-R_s-jX_s}-\frac{1}{jX_m}=\frac{1}{R_r/s+jX_r}\Rightarrow \quad (4.42)$$

$$\frac{jX_m-\left((R_{eq}-R_s)+j(X_{eq}-X_s)\right)}{jX_m\cdot\left((R_{eq}-R_s)+j(X_{eq}-X_s)\right)}=\frac{1}{R_r/s+jX_r}\Rightarrow \quad (4.43)$$

$$R_r/s+jX_r=\frac{jX_m\cdot\left((R_{eq}-R_s)+j(X_{eq}-X_s)\right)}{jX_m-\left((R_{eq}-R_s)+j(X_{eq}-X_s)\right)}\Rightarrow \quad (4.44)$$

$$R_r/s=\mathrm{Re}\left\{\frac{jX_m\cdot\left((R_{eq}-R_s)+j(X_{eq}-X_s)\right)}{jX_m-\left((R_{eq}-R_s)+j(X_{eq}-X_s)\right)}\right\}\Rightarrow \quad (4.45)$$

$$R_r/s=\frac{X_m{}^2(R_{eq}-R_s)}{(R_{eq}-R_s)^2+(X_{eq}-X_s-X_m)^2} \quad (4.46)$$

Based on the latter equation, the slip may be derived:

$$s_{estimated}=\frac{R_r\left((R_{eq,measured}-R_s)^2+(X_{eq,measured}-X_s-X_m)^2\right)}{X_m{}^2(R_{eq,measured}-R_s)} \quad (4.47)$$

As was described earlier, the slip may be estimated through the equivalent circuit of the machine in the steady-state. Moreover, the torque may be estimated through the equivalent steady-state model. In order to estimate the torque, first of all, the voltages and currents should be transformed to the αβ-domain. Then, the power at the machine terminals may be calculated.

$$\begin{cases} v_s=v_{s\alpha}+jv_{s\beta} \\ i_s=i_{s\alpha}+ji_{s\beta} \end{cases}\Rightarrow P_{terminal,measured}=3/2\,(v_{s\alpha}i_{s\alpha}+v_{s\beta}i_{s\beta}) \quad (4.48)$$

The losses in the stator may be calculated:

$$|i_s|^2=i_{s\alpha}{}^2+i_{s\beta}{}^2\Rightarrow \quad (4.49)$$

$$P_{loss,s,estimated}=3/2\,R_s|\hat{i}_s|^2 \quad (4.50)$$

Moreover, the losses in the rotor may be obtained in the following way:

$$\hat{V}_{core}=\omega_s\hat{\varphi}_{ref}\Rightarrow \quad (4.51)$$

$$P_{loss,r,estimated}=3/2\,R_r|\hat{i_r}|^2=3/2\,R_r\frac{\hat{V}_{core}^2}{(\frac{R_r}{s})^2+(\omega_sL_r)^2} \quad (4.52)$$

In addition, the core losses may be calculated.

$$\hat{V}_{core}=\omega_s\hat{\varphi}_{ref}\Rightarrow \quad (4.53)$$

$$P_{Fe,estimated}=3/2\,\frac{\hat{V}_{core}{}^2}{R_m} \quad (4.54)$$

So, the total losses and the shaft power may be calculated as:

$$\begin{cases} P_{loss,estimated}=P_{loss,s,estimated}+P_{loss,r,estimated}+P_{Fe,estimated} \\ P_{shaft,estimated}=P_{terminal,measured}+P_{loss,estimated} \end{cases} \quad (4.55)$$

The estimated value of the shaft power should be passed through a low-pass-filter in order to remove the high-frequency components as the controller is designed only to respond to slow variations of the wind speed and not the high-frequency fluctuating components and also due to the fact that the controller is designed based on the steady-state model of the induction machine. The time constant of the low-pass-filter may be selected manually. If the models of other losses are available which make it possible to calculate them only from the voltage and the current at the terminals, they could be included in the equation (4.55) as well. And finally, the torque on the shaft may be calculated as:

$$\begin{cases} \omega_{r,estimated} = (1 - s_{estimated})\omega_s \\ T_{shaft,estimated} = {}^{n_p P_{shaft,estimated}}/_{\omega_{r,estimated}} \end{cases} \quad (4.56)$$

ω_r is already estimated and available from the previous part. The estimated value of the torque should also be passed through a low-pass-filter due to the same reasons as the estimated value of the shaft power should be passed through a low-pass-filter.

Guidelines for the inclusion of the transformer and the connection cable in the control strategy

The wind turbine system design which is used in the centralized control strategy is nearly the same as a fixed-speed wind turbine system design but it is operated in a similar fashion to a variable-speed wind turbine system design through changing the frequency of the offshore grid in the HVDC station. Similar to the case of a fixed-speed offshore grid, there will be transformers required in each wind turbine unit in order to step up the voltage and reduce the current and the associated losses. Moreover, there will be undersea cables required in order to connect the wind turbines to the HVDC station. In this thesis work, it is assumed that the wind turbines are connected radially to the HVDC station. Figure 3.6 shows the simplified model of a power transformer similar to the ones used in the wind turbines and Figure 3.8 shows the equivalent circuit of a connection cable. The equivalent circuit of a connection cable, a transformer and a wind turbine generator is demonstrated in Figure 4.2. It should be noted that the cable impedance is also transferred to the secondary side of the transformer for simplification purposes. In order to prevent complexity in the calculations, the cable impedance should be lumped into the impedance of the primary side of the transformer.

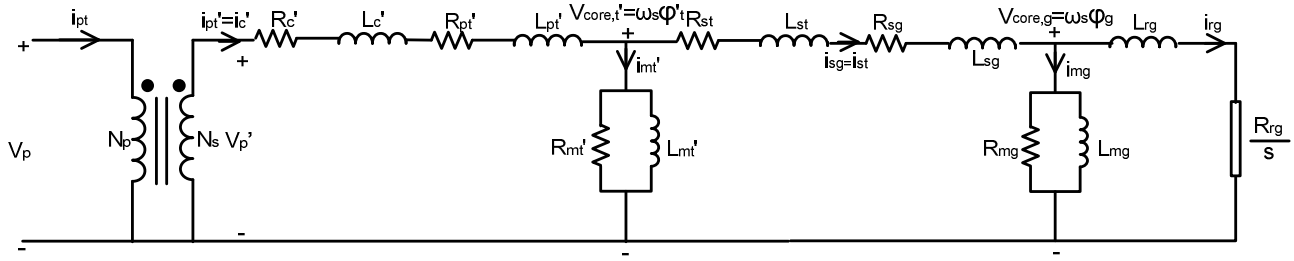

Figure 4.2 – The cable, the transformer and the generator of a wind turbine

Under such circumstances, based on the actual flux in the machine which depends on the $V_{core,g} = \varphi_g \omega_s$, the slip will be determined based on the torque on the shaft of the generator. In the same manner as was described earlier, the rotor current i_{rg} may be determined and nearly all other state variables in the circuit are based on the rotor current. Moreover, the magnetizing current of the

machine may be determined based on the $V_{core,g} = \varphi_g \omega_s$. Using the same principles as before, the voltage which is required to be applied to the input of the transformer may be derived. In the following formulas, the prime signs over the parameters which have been transferred from the primary side of the transformer to the secondary side have been omitted.

$$I_{sg} = \frac{V_{core,g}}{Z_{eq}} = \frac{V_{core,g}}{jX_{mg} \| R_{mg} \| \left({}^{R_{rg}}/_{S} + jX_{rg} \right)} \tag{4.57}$$

$$V_{core,t} = \left(\left(R_{st} + R_{sg} \right) + j\left(X_{st} + X_{sg} \right) \right) I_{sg} + V_{core,g} \tag{4.58}$$

$$I_{pt} = \frac{V_{core,t}}{jX_{mt} \| R_{mt} \| \left(R_{st} + R_{sg} + j\left(X_{st} + X_{sg} \right) + jX_{mg} \| R_{mg} \| \left({}^{R_{rg}}/_{S} + jX_{rg} \right) \right)} \tag{4.59}$$

$$V_{pt} = \left(R_{pt} + jX_{pt} \right) I_{pt} + V_{core,t} \tag{4.60}$$

An attempt to obtain a single formula with the generator flux as input and the primary voltage of the transformer as output may be made.

$$V_{core,g} = \omega_s \varphi_{g,ref} \tag{4.61}$$

$$V_{core,t} = V_{core,g} \left(1 + \frac{\left(R_{st} + R_{sg} \right) + j\left(X_{st} + X_{sg} \right)}{jX_{mg} \| R_{mg} \| \left({}^{R_{rg}}/_{S} + jX_{rg} \right)} \right) \tag{4.62}$$

$$V_{pt} = V_{core,t} (1 + \frac{\left(R_{pt} + jX_{pt} \right)}{jX_{mt} \| R_{mt} \| \left(R_{st} + R_{sg} + j\left(X_{st} + X_{sg} \right) + jX_{mg} \| R_{mg} \| \left({}^{R_{rg}}/_{S} + jX_{rg} \right) \right)}) \tag{4.63}$$

The mentioned formula will lead to the full compensation of the voltage change over the impedances which exist from the HVDC station to the core of the generator of the wind turbine. Moreover, the formula which had been derived in order to estimate the slip from the voltage and the current at the HVDC station may be generalized in order to include the transformer and the cable.

$$Z_{eq}(\mathrm{s}) = R_{pt} + jX_{pt} + jX_{mt} \parallel R_{mt} \parallel \left(R_{st} + R_{sg} + j\left(X_{st} + X_{sg} \right) + jX_{mg} \parallel R_{mg} \parallel \left({}^{R_{rg}}/_{S} + jX_{rg} \right) \right) \tag{4.64}$$

By continuously measuring the Z_{eq} in the HVDC station after transformation of the inverted voltage and the passing current into the $\alpha\beta$-domain, the controller may estimate the slip and all other corresponding variables. In order to include the transformer in the loss minimization process, a precise method and an approximate method may be used. The approximate method is based on moving the subcircuit representing the core of the transformer in parallel to the subcircuit representing the core of the generator. By doing this, the circuit representing the cable, the transformer and the generator may be simplified to the case of a single wind turbine and the simple formulas derived earlier may be used. Figure 4.3 demonstrates the approximate equivalent circuit which is needed to include the transformer in the loss minimization process.

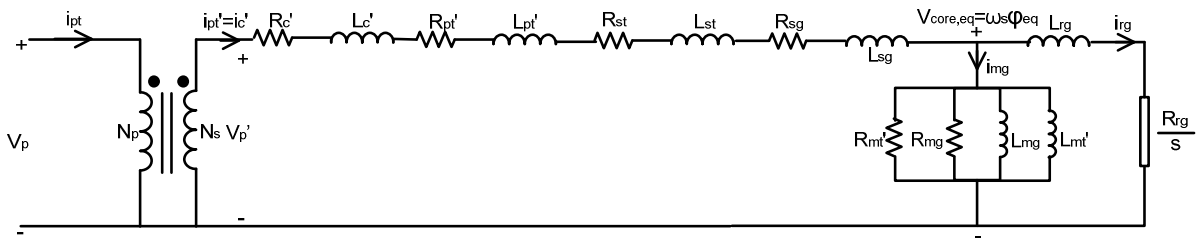

Figure 4.3 – Approximate equivalent circuit of the cable, the transformer and the generator of a wind turbine in order to be used in loss minimization process

Based on this approximate method, all the resistances and the inductances may be lumped together so that a circuit similar to that of an induction generator may be obtained and the previous formulas may be used. On the other hand, a more sophisticated formula without this approximation may be derived. In order to calculate the optimum flux level for the generator and the transformer, an approach similar to the one taken in order to derive the optimum flux formula in the case of a single turbine without the transformer should be taken. Figure 4.2 should be considered again. First of all, the magnitudes of the currents in different branches should be determined.

$$\begin{cases} |I_{rg}| \sim \frac{P_m}{3V_{core,g}} \\ |I_{mg}| \sim \frac{V_{core,g}}{X_{mg}} \end{cases} \tag{4.65}$$

$$\begin{cases} |I_{sg}|^2 \sim |I_{rg}|^2 + |I_{mg}|^2 \\ |I_{sg}|^2 \sim \frac{{P_m}^2}{9{V_{core,g}}^2} + \frac{{V_{core,g}}^2}{{X_{mg}}^2} \end{cases} \tag{4.66}$$

$$\begin{cases} {V_{core,t}}^2 \sim (V_{core,g} + (R_{st} + R_{sg})|I_{rg}|)^2 + ((X_{st} + X_{sg})|I_{mg}|)^2 \\ {V_{core,t}}^2 \sim (V_{core,g} + (R_{st} + R_{sg})\frac{P_m}{3V_{core,g}})^2 + ((X_{st} + X_{sg})\frac{V_{core,g}}{X_{mg}})^2 \\ {V_{core,t}}^2 = {V_{core,g}}^2 + (R_{st} + R_{sg})^2 \frac{{P_m}^2}{9{V_{core,g}}^2} + \frac{2}{3}(R_{st} + R_{sg})P_m + (X_{st} + X_{sg})^2 \frac{{V_{core,g}}^2}{{X_{mg}}^2} \\ {V_{core,t}}^2 = \left(1 + \left(\frac{X_{st}+X_{sg}}{X_{mg}}\right)^2\right){V_{core,g}}^2 + (R_{st} + R_{sg})^2 \frac{{P_m}^2}{9{V_{core,g}}^2} + \frac{2}{3}(R_{st} + R_{sg})P_m \end{cases} \tag{4.67}$$

$$|I_{mt}| \sim \frac{V_{core,t}}{X_{mt}} \tag{4.68}$$

$$\begin{cases} |I_{pt}|^2 \sim |I_{rg}|^2 + (|I_{mg}| + |I_{mt}|)^2 \\ |I_{pt}|^2 \sim \left(\frac{P_m}{3V_{core,g}}\right)^2 + \left(\frac{V_{core,g}}{X_{mg}} + \frac{V_{core,t}}{X_{mt}}\right)^2 \\ |I_{pt}|^2 \sim \frac{{P_m}^2}{9{V_{core,g}}^2} + \frac{{V_{core,g}}^2}{{X_{mg}}^2} + \frac{2{V_{core,g}}^2}{X_{mg}X_{mt}} + \frac{{V_{core,t}}^2}{{X_{mt}}^2} \\ |I_{pt}|^2 \sim \frac{{P_m}^2}{9{V_{core,g}}^2} + \left(\frac{1}{{X_{mg}}^2} + \frac{2}{X_{mg}X_{mt}}\right){V_{core,g}}^2 + \frac{{V_{core,t}}^2}{{X_{mt}}^2} \end{cases} \tag{4.69}$$

$$\left|\mathrm{I_{pt}}\right|^2 \sim \frac{\mathrm{P_m}^2}{9\mathrm{V_{core,g}}^2} + \left(\frac{1}{\mathrm{X_{mg}}^2} + \frac{2}{\mathrm{X_{mg}X_{mt}}}\right)\mathrm{V_{core,g}}^2 + \frac{1}{\mathrm{X_{mt}}^2}\left(\left(1 + \left(\frac{\mathrm{X_{st}+X_{sg}}}{\mathrm{X_{mg}}}\right)^2\right)\mathrm{V_{core,g}}^2 + \left(\mathrm{R_{st}} + \mathrm{R_{sg}}\right)^2 \frac{\mathrm{P_m}^2}{9\mathrm{V_{core,g}}^2} + \frac{2}{3}\left(\mathrm{R_{st}} + \mathrm{R_{sg}}\right)\mathrm{P_m}\right) \quad (4.70)$$

$$\left|\mathrm{I_{pt}}\right|^2 \sim \frac{\mathrm{P_m}^2}{9}\left(1 + \frac{\left(\mathrm{R_{st}+R_{sg}}\right)^2}{\mathrm{X_{mt}}^2}\right)\frac{1}{\mathrm{V_{core,g}}^2} + \left(\frac{1}{\mathrm{X_{mg}}^2} + \frac{2}{\mathrm{X_{mg}X_{mt}}} + \frac{1+\left(\frac{\mathrm{X_{st}+X_{sg}}}{\mathrm{X_{mg}}}\right)^2}{\mathrm{X_{mt}}^2}\right)\mathrm{V_{core,g}}^2 + \frac{2}{3\mathrm{X_{mt}}^2}\left(\mathrm{R_{st}} + \mathrm{R_{sg}}\right)\mathrm{P_m} \quad (4.71)$$

Then, the total losses may be determined. The total loss formula should be arranged in a format ready for the minimization process.

$$P_{loss} = P_{rg} + P_{st-sg} + P_{c-pt} + P_{Fe,g} + P_{Fe,t} \quad (4.72)$$

$$P_{loss} = 3R_{rg}\frac{{P_m}^2}{9{V_{core,g}}^2} + 3\left(R_{st} + R_{sg}\right)\left\{\frac{\mathrm{P_m}^2}{9\mathrm{V_{core,g}}^2} + \frac{\mathrm{V_{core,g}}^2}{\mathrm{X_{mg}}^2}\right\} + 3\left(R_c + R_{pt}\right)\left\{\frac{\mathrm{P_m}^2}{9}\left(1 + \frac{\left(\mathrm{R_{st}+R_{sg}}\right)^2}{\mathrm{X_{mt}}^2}\right)\frac{1}{\mathrm{V_{core,g}}^2} + \left(\frac{1}{\mathrm{X_{mg}}^2} + \frac{2}{\mathrm{X_{mg}X_{mt}}} + \frac{1+\left(\frac{\mathrm{X_{st}+X_{sg}}}{\mathrm{X_{mg}}}\right)^2}{\mathrm{X_{mt}}^2}\right)\mathrm{V_{core,g}}^2 + \frac{2}{3\mathrm{X_{mt}}^2}\left(\mathrm{R_{st}} + \mathrm{R_{sg}}\right)\mathrm{P_m}\right\} + 3\frac{{V_{core,g}}^2}{R_{mg}} + \frac{3}{R_{mt}}\left\{\left(1 + \left(\frac{\mathrm{X_{st}+X_{sg}}}{\mathrm{X_{mg}}}\right)^2\right)\mathrm{V_{core,g}}^2 + \left(\mathrm{R_{st}} + \mathrm{R_{sg}}\right)^2\frac{\mathrm{P_m}^2}{9\mathrm{V_{core,g}}^2} + \frac{2}{3}\left(\mathrm{R_{st}} + \mathrm{R_{sg}}\right)\mathrm{P_m}\right\} \quad (4.73)$$

$$P_{loss} = 3\mathrm{V_{core,g}}^2 \times \left\{\frac{\left(R_{st}+R_{sg}\right)}{\mathrm{X_{mg}}^2} + \left(R_c + R_{pt}\right)\left(\frac{1}{\mathrm{X_{mg}}^2} + \frac{2}{\mathrm{X_{mg}X_{mt}}} + \frac{1+\left(\frac{\mathrm{X_{st}+X_{sg}}}{\mathrm{X_{mg}}}\right)^2}{\mathrm{X_{mt}}^2}\right) + \frac{1}{R_{mg}} + \frac{1}{R_{mt}}\left(1 + \left(\frac{\mathrm{X_{st}+X_{sg}}}{\mathrm{X_{mg}}}\right)^2\right)\right\} + \frac{3}{\mathrm{V_{core,g}}^2} \times \left\{R_{rg}\frac{{P_m}^2}{9} + \left(R_{st} + R_{sg}\right)\frac{\mathrm{P_m}^2}{9} + \left(R_c + R_{pt}\right)\left(1 + \frac{\left(\mathrm{R_{st}+R_{sg}}\right)^2}{\mathrm{X_{mt}}^2}\right)\frac{\mathrm{P_m}^2}{9} + \frac{\left(\mathrm{R_{st}+R_{sg}}\right)^2}{R_{mt}}\frac{\mathrm{P_m}^2}{9}\right\} + 3\left(R_c + R_{pt}\right)\frac{2}{3\mathrm{X_{mt}}^2}\left(\mathrm{R_{st}} + \mathrm{R_{sg}}\right)\mathrm{P_m} + \frac{3}{R_{mt}}\frac{2}{3}\left(\mathrm{R_{st}} + \mathrm{R_{sg}}\right)\mathrm{P_m} \quad (4.74)$$

The latter equation may be used to obtain the optimum voltage of the core of the generator.

$$\mathrm{A} = 3\left\{\frac{\left(R_{st}+R_{sg}\right)}{\mathrm{X_{mg}}^2} + \left(R_c + R_{pt}\right)\left(\frac{1}{\mathrm{X_{mg}}^2} + \frac{2}{\mathrm{X_{mg}X_{mt}}} + \frac{1+\left(\frac{\mathrm{X_{st}+X_{sg}}}{\mathrm{X_{mg}}}\right)^2}{\mathrm{X_{mt}}^2}\right) + \frac{1}{R_{mg}} + \frac{1}{R_{mt}}\left(1 + \left(\frac{\mathrm{X_{st}+X_{sg}}}{\mathrm{X_{mg}}}\right)^2\right)\right\} \quad (4.75)$$

$$B = 3\left\{R_{rg}\frac{P_m^{\,2}}{9} + \left(R_{st}+R_{sg}\right)\frac{P_m^{\,2}}{9} + \left(R_c+R_{pt}\right)\left(1+\frac{\left(R_{st}+R_{sg}\right)^2}{X_{mt}^{\,2}}\right)\frac{P_m^{\,2}}{9} + \frac{\left(R_{st}+R_{sg}\right)^2}{R_{mt}}\frac{P_m^{\,2}}{9}\right\} \quad (4.76)$$

$$C = 3\left(R_c+R_{pt}\right)\frac{2}{3X_{mt}^{\,2}}\left(R_{st}+R_{sg}\right)P_m + \frac{3}{R_{mt}}\frac{2}{3}\left(R_{st}+R_{sg}\right)P_m \quad (4.77)$$

$$P_{loss} = V_{core,g}^{\,2} \times A + \frac{1}{V_{core,g}^{\,2}} \times B + C \quad (4.78)$$

And, in the end:

$$\Rightarrow \frac{dP_{loss}}{dV_{core,g}} = 2AV_{core,g} - 2BV_{core,g}^{\,-3} = 0 \quad (4.79)$$

$$V_{core,g} = \sqrt[4]{\frac{B}{A}} = \sqrt[4]{\frac{\left\{R_{rg}\frac{P_m^{\,2}}{9}+\left(R_{st}+R_{sg}\right)\frac{P_m^{\,2}}{9}+\left(R_c+R_{pt}\right)\left(1+\frac{\left(R_{st}+R_{sg}\right)^2}{X_{mt}^{\,2}}\right)\frac{P_m^{\,2}}{9}+\frac{\left(R_{st}+R_{sg}\right)^2 P_m^{\,2}}{R_{mt}\quad 9}\right\}}{\left\{\frac{\left(R_{st}+R_{sg}\right)}{X_{mg}^{\,2}}+\left(R_c+R_{pt}\right)\left(\frac{1}{X_{mg}^{\,2}}+\frac{2}{X_{mg}X_{mt}}+\frac{1+\left(\frac{X_{st}+X_{sg}}{X_{mg}}\right)^2}{X_{mt}^{\,2}}\right)+\frac{1}{R_{mg}}+\frac{1}{R_{mt}}\left(1+\left(\frac{X_{st}+X_{sg}}{X_{mg}}\right)^2\right)\right\}}} \quad (4.80)$$

Based on the latter equation, the optimum flux in the generator may be calculated and using the other formulas which had been derived earlier, all other required variables may be obtained.

4.2. The case of an offshore wind farm

In an offshore wind farm whose energy is transported through an HVDC link, there is possibility for the offshore wind farm grid to have a voltage and frequency different from those of the onshore grid. As the frequency of the electric voltage applied to an induction machine has a significant impact on the speed of the machine and the magnitude of the electric voltage applied to an induction machine has an important impact on its flux and the losses, the controllers in the transmitting side of the HVDC station may manipulate the frequency and the voltage of the offshore grid in order to control the behaviour of the induction machines in the wind turbines and improve it. Wind turbine models are fairly complex and because of this, simulations usually take long times and need a lot of computer resources. The problem becomes more serious when the study of a wind farm as a whole is performed. Usually all the wind turbines used in a wind farm are of the same type and from the same manufacturer. Moreover, due to high levels of coherence among the wind speeds at different locations of a wind farm, the wind speed and consequently the shaft torques of the wind turbines do not differ widely in different point of the wind farm. Also, temperature and weather conditions are approximately the same in different points of a wind farm [14]. Such facts may be used to simplify the wind farm model for power system studies. An acceptable approximation may be using a single wind turbine model instead of all wind turbines in a wind farm. As all the wind turbines in a wind farm are working at operating points very near each other, this model leads to good results which conform to measurements [15]. Figure 4.4 demonstrates the aggregration of a wind farm and simplification of wind farm studies through assuming the whole wind farm as a single wind turbine system. It should

be noted that in the case of a wind farm, also the transformer model should be integrated into the wind turbine model. In order to do this the transformer equivalent series impedance should be added to the generator stator impedance so that the voltage drop over the transformer gets compensated. Moreover, the impedance representing the core of the transformer should be considered in parallel to the core impedance of the generator.

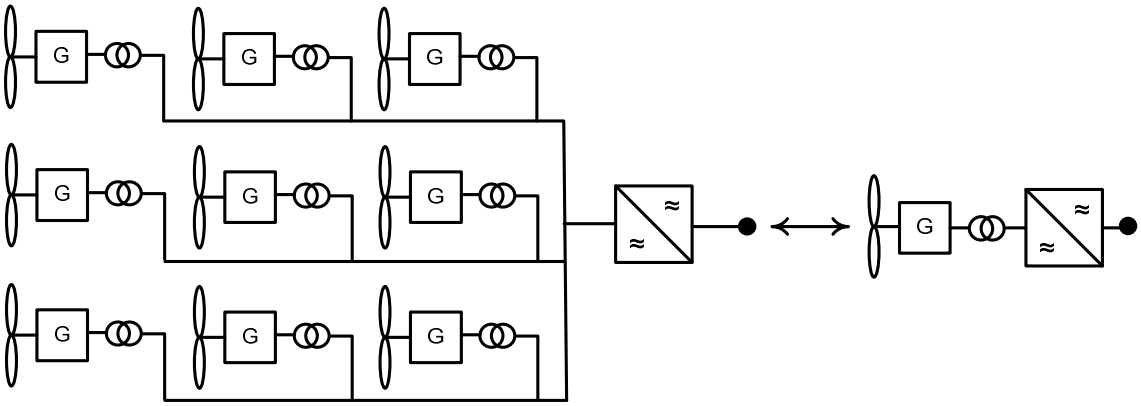

Figure 4.4 – Simplification of a wind farm into a single wind turbine unit

The formulas and the strategy developed so far may be generalized from a single wind turbine unit to the case of a wind farm. In the case of a wind farm, there is a possibility of simplifying the wind turbines through removing all of the individual speed control systems including the individual converters of all wind turbines and employing a centralized speed control mechanism instead along with a much larger converter in the HVDC station. Under such circumstances, none of the wind turbines will operate at the optimum working point and also none of them will have maximum aerodynamic efficiency. On the other hand, the application of the proposed control system for the centralized control of a wind farm is an improvement to the fixed-speed wind farm situation. In the wind farm case, different wind turbines will be exposed to different wind speeds, so, the power output from them will be different. In such cases, an average power may be used instead. In fact, mathematically, there is no reasonable way to access the individual turbine operation data.

$$P_{avg} = \frac{\sum_{i=1}^{i=N} P_i}{N} = \frac{P_{HVDC-station}}{N} \tag{4.81}$$

In order to perform the centralized speed and flux level control in a wind farm, the controller in the HVDC station should measure the power input from the wind farm grid and perform the calculations of the previous section on an equivalent induction machine. Figure 4.5 demonstrates the general control strategy for the case of a wind farm.

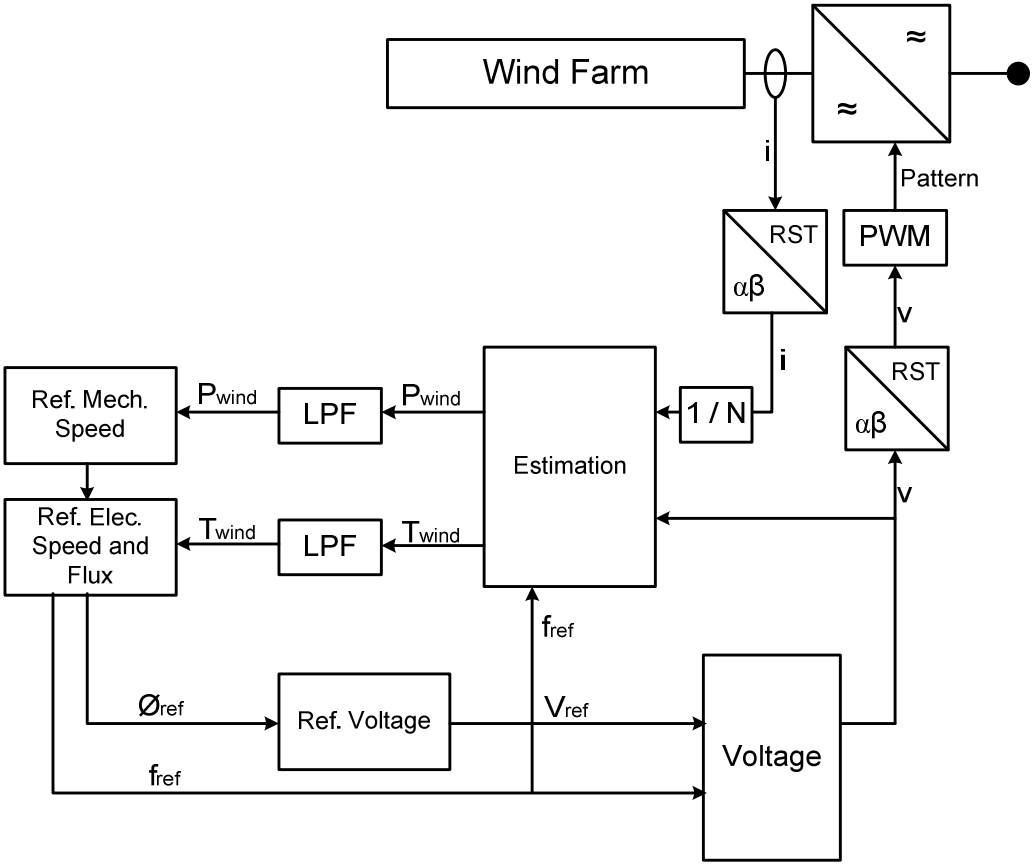

Figure 4.5 – The control strategy for the case of a wind farm

5. Evaluation of the centralized control strategy

5.1. Efficiency study

One of the key goals in the manipulation of the characteristics of the custom offshore grid is to increase the efficiencies of the wind turbines. In order to achieve this, the operation of the induction machine while connected to different voltage level references should be compared. Three possible strategies are (i) the constant rated flux method, (ii) the numerical-based minimum loss method and (iii) approximatation-based minimum loss method. The minimum loss strategies had been derived in the previous chapter. In order to get insight into the process of loss minimization, the total losses, the efficiency, the terminal voltage and the synchronous frequency of a wind turbine for the case of wind speed equal to 6 m/s for the different flux levels has been plotted in Figures 5.1.

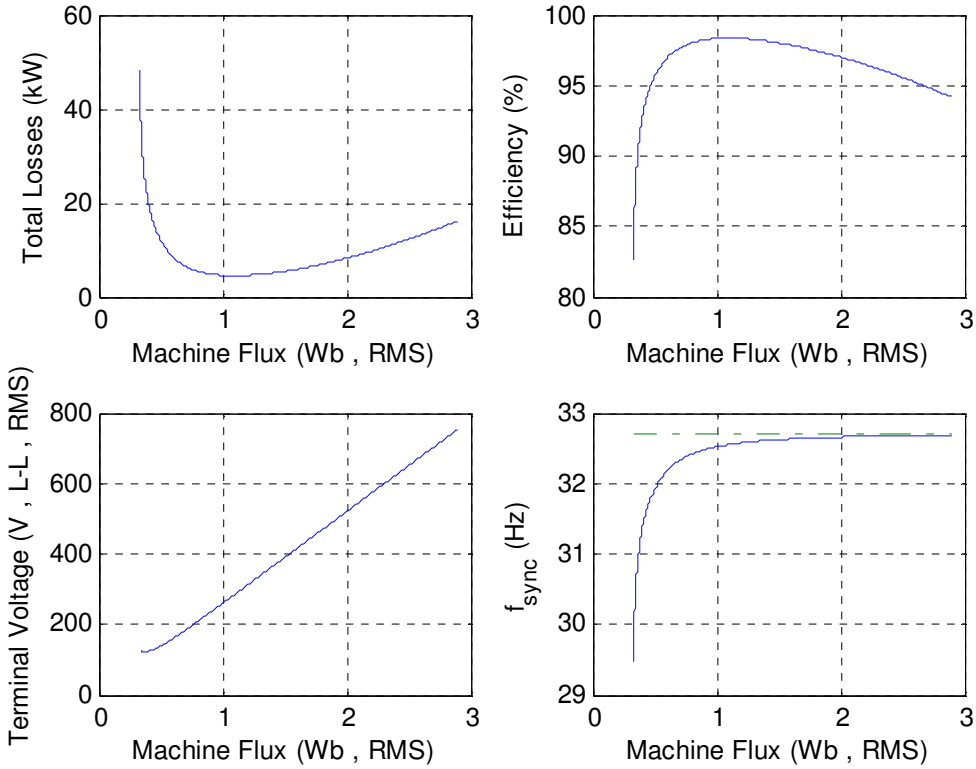

Figure 5.1 – Analysis of the case of the wind speed equal to 6 m/s

It is observed that the losses in the machine and consequently the efficiency of the machine depends on the magnitude of the machine flux. With increasing the flux while keeping the torque and the rotor mechanical speed constant, the rotor frequency decreases and the synchrous frequency of the voltage applied to the machine gets closer to the value of the reference mechanical speed. Moreover, with increasing the flux, as the magnitude of the stator and rotor currents decrease, the losses associated with them decrease too. On the other hand, with decreasing the flux, the synchronous frequency of the voltage applied to the machine decreases. The core losses depend on the flux magnitude and the synchronous frequency, so, with decreasing the flux the core losses decrease. These two opposite trends in the machine losses variations lead to the existence of a minimum loss operating point which leads to the maximum efficiency of the machine. For any wind speed, such a minimum loss point

exists that should be chosen as the reference point for the offshore grid operation so that the efficiency of the wind turbine become maximized. The different operating points of the machine while using different flux reference methods have been plotted in Figure 5.2.

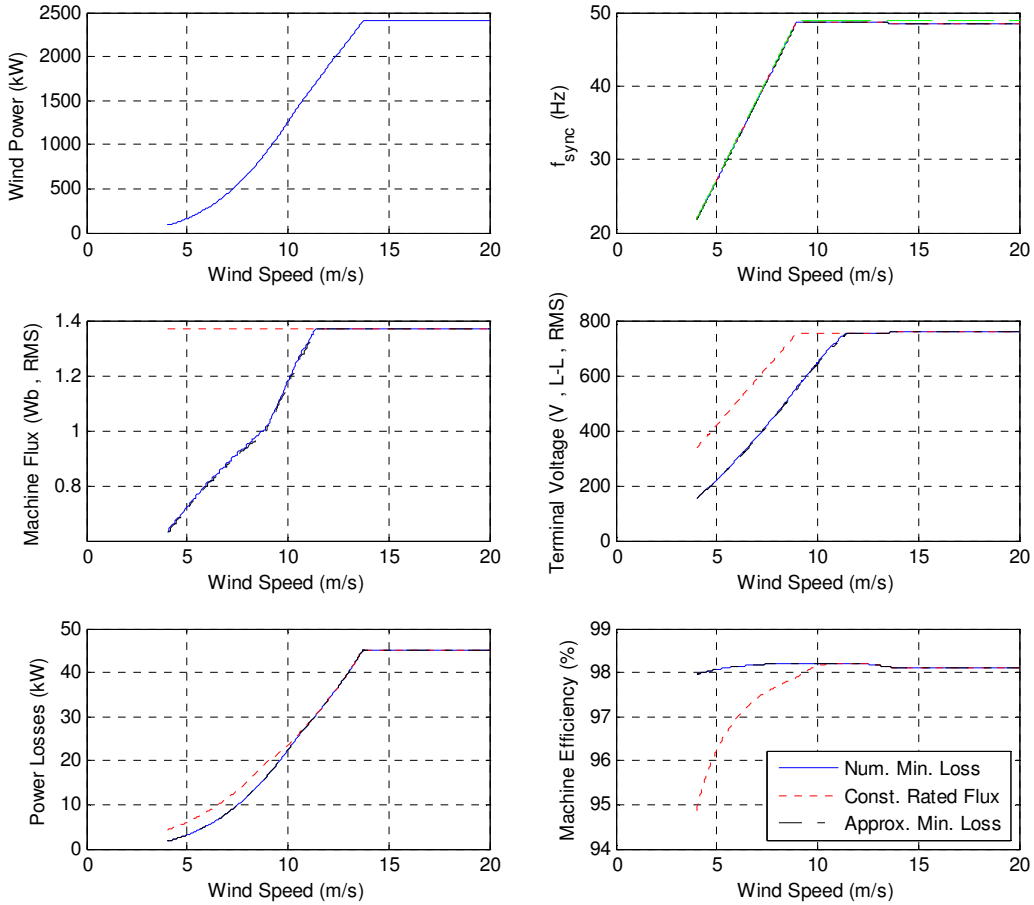

Figure 5.2 – Different flux reference methods for the wind turbine operation

The fact that the wind power is proportional to the 3rd power of the wind speed should be considered along with the cut-in and cut-out speeds of the wind turbine and the maximum power rating of the generator. The power curve of the wind turbine can be plotted considering these facts. For the wind speeds below 8 m/s, the synchrous frequency of the generator is decreased in order to maximize the wind power energy absorption. This is done based on the optimum tip-speed-ratio which leads to the maximum aerodynamic efficiency. Above the wind speed 8 m/s, it is not possible to follow the maximum aerodynamic efficiency lookup table as this will lead to the turbine speeds higher than the maximum allowed value. Also, the frequencies higher than the rated value is not allowed for the generator as the frequency-dependent losses may grow higher than the designed value and this may lead to damaging the machine. Furthermore, it is not possible to run a machine at speeds higher than the rated value as this will damage the mechanical parts. The gear-box-ratio should be chosen so that the maximum speed of the generator and the maximum speed of the turbine correspond to each other. The pole pair numbers should also be considered in choosing the gear-box-ratio. It is observed that the approximate method has appropriate conformance to the numerical loss minimization method. In the

rated-constant-flux method, the core voltage is manipulated so that the flux in the machine always remains equal to the rated designed value. In low wind speeds, this may not be optimum as it is seen in the graphs. In the loss minimization strategy, in low speeds, the flux in the machine is decreased so that the core losses decrease. This will lead to higher efficiencies of the machine as it is seen in the graphs. It should be noted that in higher wind speeds, the minimum loss method and the rated flux method lead to the same results as the voltage of the terminals of the machine may not be increased above the rated value. The fact that the machine flux graph has higher slope in the range 8 m/s ~ 12 m/s should be noted. This is because of the fact that in this region there is no change in the synchronous frequency and all the loss decrementation should be done through manipulating the flux alone while in the wind speed range 4 m/s ~ 12 m/s, the decrementation of the losses may be done also through decreasing the frequency. Due to these reasons, the approximate minimum loss method has been chosen for the simulations in the next sections.

5.2. Feasibility study

The case with a single wind turbine using the control strategy (MATLAB/Simulink)

In order to demonstrate the feasibility of the implementation of the centralized control strategy on a wind turbine, a single wind turbine with the proposed controller in action is simulated using MATLAB/Simulink. Figure 5.3 demonstrates the case setup for the simulation.

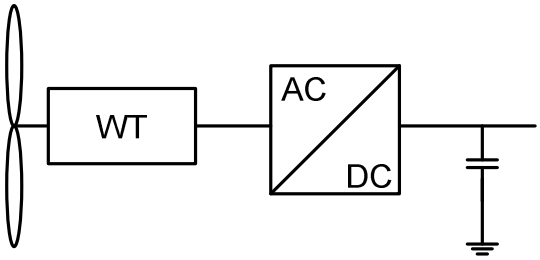

Figure 5.3 – The case setup for the simulation

The parameters used for the simulation are from a sample wind turbine whose information is included in Appendix A. The induction machine dynamic model is defined as a MATLAB s-function. The estimation subsystem is responsible for estimating the important variables, the slip and the torque. The HVDC substation subsystem will be responsible for providing the voltage to the wind turbine. In order to provide the optimum operation for the system, first of all, the optimum flux for the machine is calculated using the respective blocks. This flux is also passed to the estimator subsystem. Based on this reference flux, the voltage which is needed to be fed into the machine and also the frequency of this voltage will be calculated. The frequency should be chosen in such a way that the system follows the reference mechanical speed. In order to maximize the aerodynamic conversion efficiency, the reference speed should be changed according to the wind speed. As the wind speed is not easily measurable, another method may be used based on the setting of the reference speed based on the output power. It should be noted that in order for the block responsible for the determination of the reference speed to work correctly, the wind power may be calculated from the power from the terminals plus the power losses in the system. The steady-state equivalent model of the induction machine may be used for the loss calculations. The wind speed which is used in the simulation is

demonstrated in Figure 5.4. This wind speed transfers energy into the system through the blades. The low-speed shaft will have a speed which is plotted in Figure 5.5.

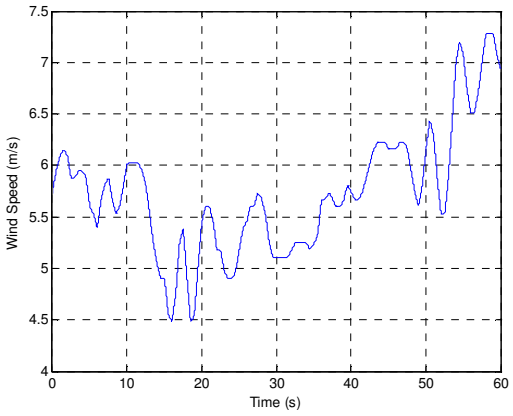

Figure 5.4 – Wind speed vs. time

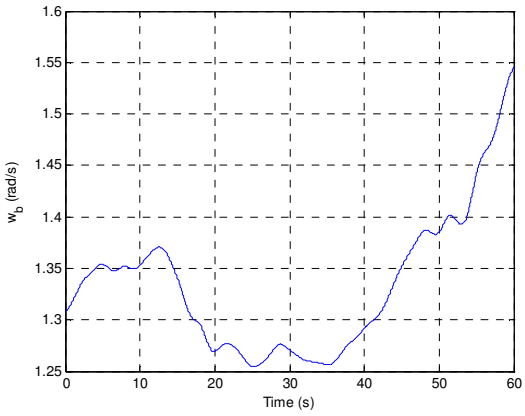

Figure 5.5 – Low-speed shaft speed vs. time

It is noted that for the higher speeds of the wind, the system has maintained a higher rotational speed in order to maximize the conversion process efficiency. The aerodynamic conversion efficiency of the simulated wind turbine is demonstrated in Figure 5.6. It is noted that the system has always maintained a good aerodynamic conversion efficiency, i.e. an efficiency over 47%. It should be considered that maximum aerodynamic efficiency which is theoretically possible is $^{9}/_{16}$ which is approximately equal to 54%. The torque on the low-speed-shaft is applied to a gear-box where it is delivered to a high-speed-shaft. The high-speed-shaft is the shaft of the generator where torque is lower. The torque on the generator is plotted in Figure 5.7.

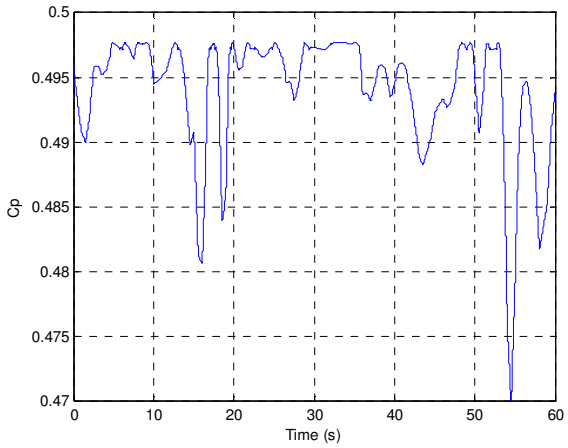

Figure 5.6 – C_p vs. time

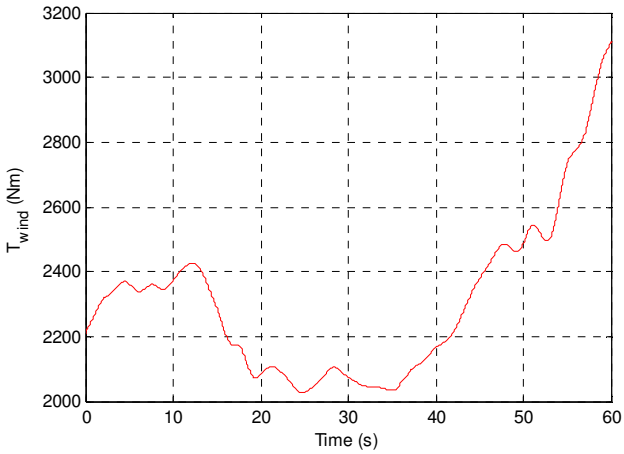

Figure 5.7 – Generator torque vs. time

The proposed controller inside the HVDC station, determines the frequency to be applied to the grid to control the speed along with the voltage which is intended to minimize the losses in the generators. The frequency and the voltage applied to the wind turbine are plotted in Figures 5.8 and 5.9 respectively. It should be noted that as the generator employed in the simulation is an induction machine and it is operated in the generator mode, the actual speed of the machine is higher than the frequency of the voltage which is applied to it.

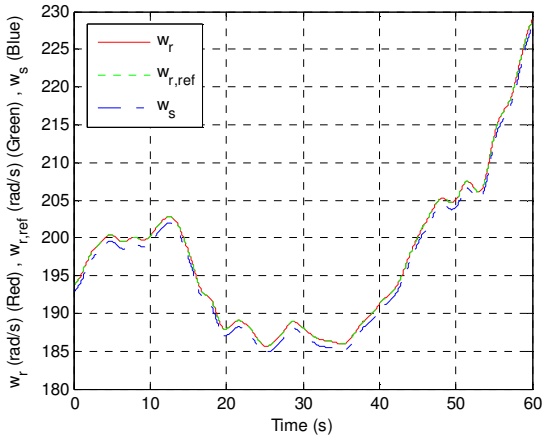

Figure 5.8 – Rotor speed, Reference speed and Applied angular frequency vs. time

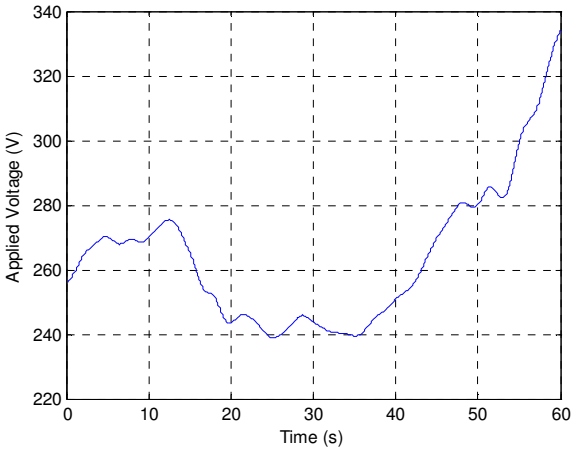

Figure 5.9 – Applied voltage vs. time

The reference flux along with the actual flux in the machine are shown in Figure 5.10. It is observed that the actual flux in the machine follows the reference flux very closely. This fact should be considered that as the wind speed and consequently the torque on the shaft decreases, the flux in the machine is decreased too. This is due to the fact that as the power transferred to the machine decreases, there is no need to maintain higher levels of flux in the machine. This helps to lower the iron losses also. In order to evaluate the effectiveness of the torque estimation process, both the actual and the estimated torques are plotted in Figure 5.11. It is observed that the estimation process has a very good precision.

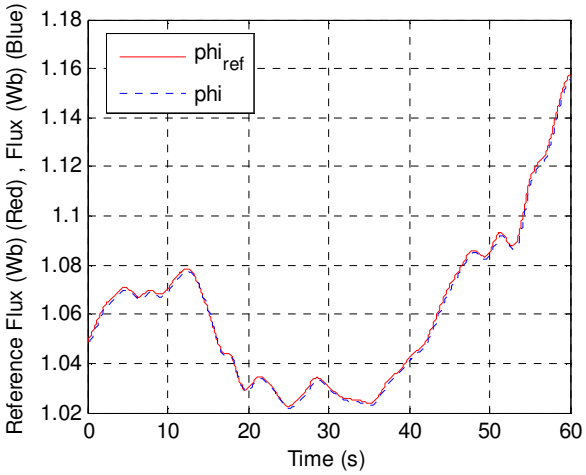

Figure 5.10– Reference flux and actual flux vs. time

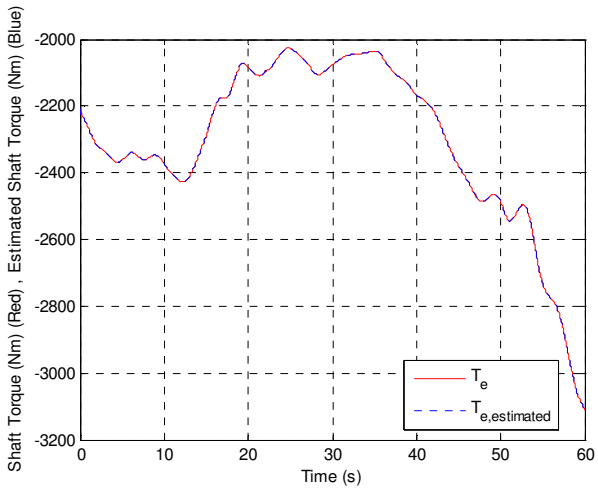

Figure 5.11 – Shaft torque and its estimated value vs. time

The facts and figures show that in the steady-state operation of an induction machine, the speed and the flux may be controlled with a negligible error. This is also the case when the machine is not in a perfect steady-state condition but rather in a very slow transient mode as in a wind turbine due to extremely high intertia. To get a further insight into the effectiveness of the proposed control method in obtaining reasonable results, Table 5.1 should be considered.

Maximum theoretical C_p for this turbine	49.77 %
Minimum C_p during operation	47.00 %
Average C_p during operation	49.48 %

Table 5.1 – Aerodynamic efficiency of the turbine

According to the previous table, very good results for the maximization of the C_p for a single wind turbine is obtained.

The case with two parallel wind turbines using the control strategy (PSCAD/EMTDC)

As was stated before, the proposed strategy may be used in a wind farm in order to remove the individual speed control mechanisms. In order to show the feasibility of such an action, the case of the parallel operation of two wind turbines is studied. Figure 5.12 demonstrates the case setup for the simulation.

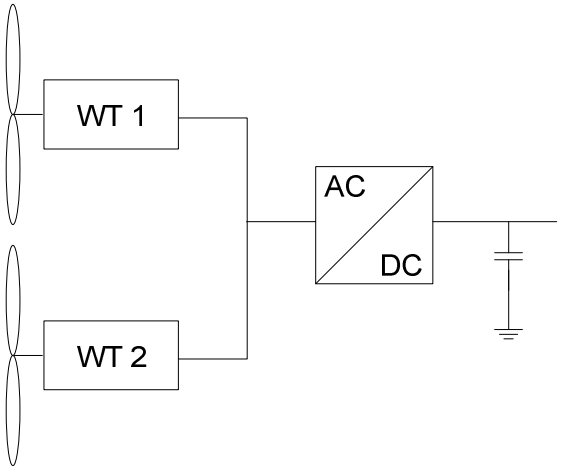

Figure 5.12 – The case setup for the simulation

In such a configuration, two wind turbines are defined in PSCAD/EMTDC along with an implementation of the proposed controller for the HVDC station. The turbines are assumed to be working in parallel and the controller system continuously senses the current passing through the HVDC station and takes consequent actions. PSCAD/EMTDC simplifies some parts of the simulation by providing built-in models for many parts of the system like the multi-mass interface and the induction generator. On the other hand, all MATLAB/Simulink subroutines and diagrams are to be re-implemented in PSCAD/EMTDC. Moreover, as the block diagrams drawn in PSCAD/EMTDC is translated into FORTRAN code and compiled, the method of drawning the blocks may be very tricky and the possibility of loss of data due to round-off errors while working with very large or very small numbers should be considered. This is the case with this simulation which although the simulation is straightforward, it may get very difficult and time-consuming to implement. In order to study the parallel operation of the turbines, 60 seconds of the operation of the system is simulated and studied. Two sequences of wind speeds data have been fed into a lookup table of the PSCAD/EMTDC which have been demonstrated in Figure 5.13. The mentioned sequences of the wind speeds have the good characteristic that until 35th second of operation, they are very close to each other, while after that

instant of time, they deviate from each other a lot. These two sequences have been deliberately chosen to demonstrate the relation between the wind farm efficiency and the variation among different wind speeds of the wind turbines in the farm. It should be pointed out that in reality it is impossible to track the wind speed. As was mentioned before, based on the reference mechanical speed needed and the estimated torque of the machine, the proposed controller manipulates the frequency of the offshore grid in order to obtain a desirable aerodynamic efficiency. The reference frequency along with the applied frequency to the grid and the actual speeds of the two turbines have been demonstrated in Figure 5.14.

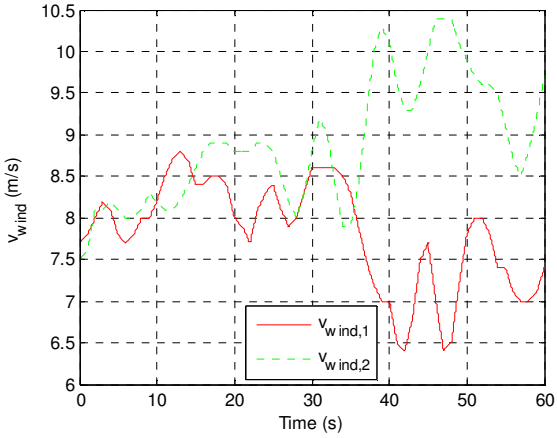

Figure 5.13 – Wind speeds of the turbines vs. time

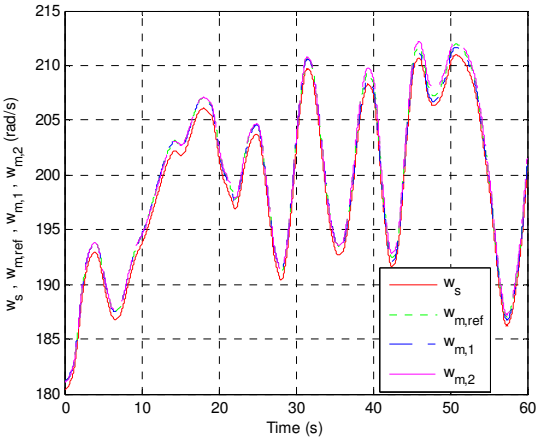

Figure 5.14 – Applied frequency, Reference speed and Actual turbine speeds vs. time

As was noted before, as the induction machines are operated within the generator region, actually the speeds of the machines will be higher than the applied frequency. None of the wind turbines operate at the maximum efficiency while the efficiency of the wind farm as a whole is maximum, considering available equipment, i.e. a single power electronics converter in the HVDC station only. The voltage which is applied to the grid, which is also dependant on the load, is demonstrated in Figure 5.15. Based on the λ and corresponding values of β, the aerodynamic efficiencies of the wind turbines have been plotted in Figure 5.16.

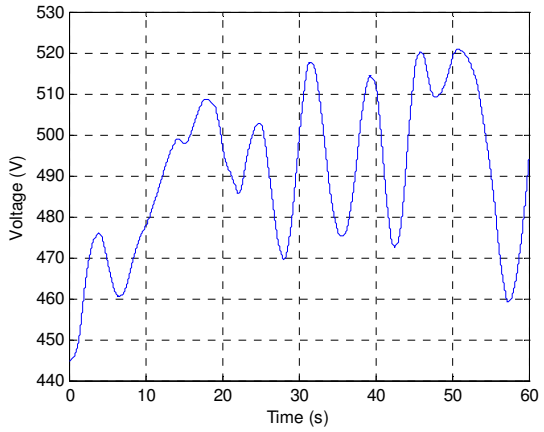

Figure 5.15 – Applied voltage to the wind farm grid vs. time

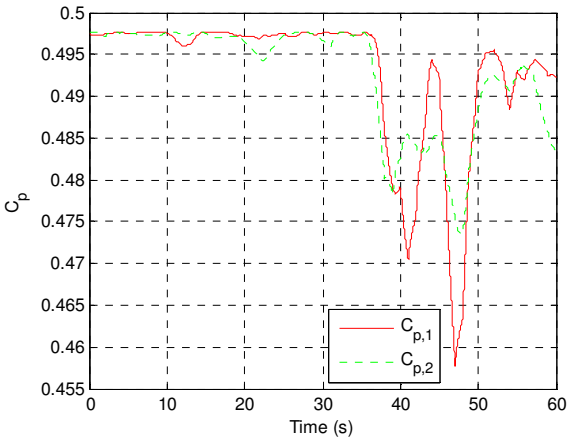

Figure 5.16 – Aerodynamic efficiencies of the turbines vs. time

It should be noted that in the first 35 seconds of the system operation in which the wind speeds had close values, the aerodynamic efficiencies of the wind turbines were very high and almost the maximum possible while in the next instants of the operation when the wind speed values had much more different values, the efficiencies were decreased. This is a general concept in the centralized wind farm control that the controller in the HVDC station will have a more accurate operation when the deviation of the wind speeds from each other are low. Moreover, the power generated by the wind turbines have been demonstrated in Figure 5.17. It should be noted that although in the region where two wind speeds have high variances, the efficiency of the turbine with the higher wind speed is decreased, the power produced by it is increased as the produced power is related to cube of the wind speed value.

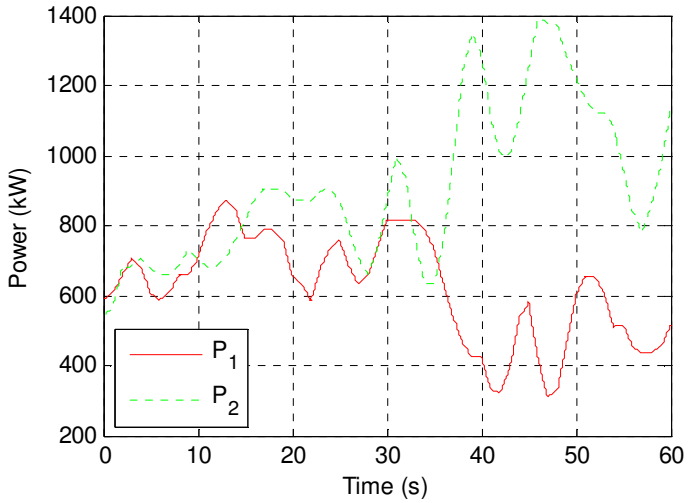

Figure 5.17 – Output powers from the wind turbines vs. time

In order to evaluate the effectiveness of the proposed control strategy in the operation of two parallel turbines, Figures 5.18 should be considered.

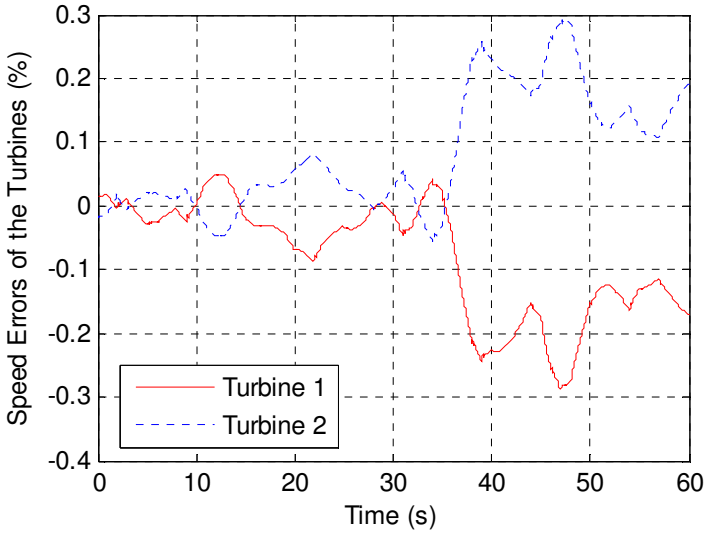

Figure 5.18 – Speed errors of the turbines vs. time

It should be noted that until the 35th second of the operation the speed error was nearly negligible due to the fact that both the wind speeds of the turbines and consequently the torques were near each other and with an effective slip compensation, the induction machines may be set exactly to the desired reference. On the other hand, after the 35th second of the operation, the wind speeds deviate from each other and the torque which is compensated is not equal to that of any of the wind turbines. So, there will be an speed error. This speed error depends on the deviation between the wind speeds. As the C_p curve is not an steep one, especially near the maximum point, the consequent deviations in the C_p will not be considerable. Tables 5.2 and 5.3 show the speed controlling capabilities of the centralized control method.

Maximum speed error (1st turbine)	0.2889 %
Average speed error (1st turbine)	0.0884 %

Table 5.2 – Speed controlling capabilities for the first turbine with the double-turbine case

Maximum speed error (2nd turbine)	0.2922 %
Average speed error (2nd turbine)	0.0899 %

Table 5.3 – Speed controlling capabilities for the second turbine with the double-turbine case

It should be noted that the speed error is very low and the speed control mechanism can be considered effective. Tables 5.4 and 5.5 show the aerodynamic efficiencies in the double-turbine case.

Minimum C_p (1st turbine)	45.77 %
Average C_p (1st turbine)	49.29 %

Table 5.4 – 1st turbine C_p capabilities

Minimum C_p (2nd turbine)	47.35 %
Average C_p (2nd turbine)	49.27 %

Table 5.5 – 2nd turbine C_p capabilities

It is noted that both turbines have operated on an acceptable efficiency on average during the period of the simulation. In order to get an insight into the effect of the wind speeds being close to each other the tables 5.6~5.9 should be considered.

Minimum C_p (1st turbine)	49.61 %
Average C_p (1st turbine)	49.74 %

Table 5.6 – 1st turbine C_p capabilities (0-35s)

Minimum C_p (1st turbine)	48.66 %
Average C_p (1st turbine)	45.77 %

Table 5.7 – 1st turbine C_p capabilities (35s-60s)

Minimum C_p (2nd turbine)	49.43 %
Average C_p (2nd turbine)	49.71 %

Table 5.8 – 2nd turbine C_p capabilities (0-35s)

Minimum C_p (2nd turbine)	47.35 %
Average C_p (2nd turbine)	48.65 %

Table 5.9 – 2nd turbine C_p capabilities (35s-60s)

It is observed that in the period 0-35s both the turbines have efficiencies near the maximum value while in the period 35s-60s the efficiencies are slightly lower. This is due to the deviations in the wind speeds leading to different torques as was described earlier. It should be noted that because of the characteristics of the C_p curve, even though the wind speeds are different, the decrementation in the C_p value is negligible.

5.3. Energy production study

Time-series analysis of one hour operation of a 2x2 offshore wind farm

In the previous section, the feasibility of the proposed control strategy with a single wind turbine and two wind turbines in parallel was studied. The results showed that the formulas and strategies described actually converge and work. Also, the feasibility of the application of this method with the case of multiple wind turbines, i.e. a wind farm had been demonstrated. In this simulation, a set of four wind turbines with different sets of wind speeds are assumed to be working in parallel while the specified controller is in action in the HVDC station. The produced energy of each individual turbine is measured and compared to the situation in which individual speed control were used. Figure 5.19 shows the case setup for this simulation.

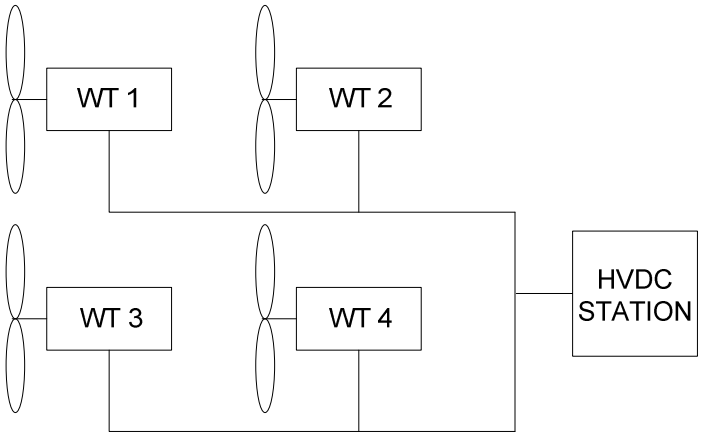

Figure 5.19 – The case setup for the simulation

Figure 5.20 shows the sequence of wind speeds which were used to perform the simulation in the duration of 1 hour.

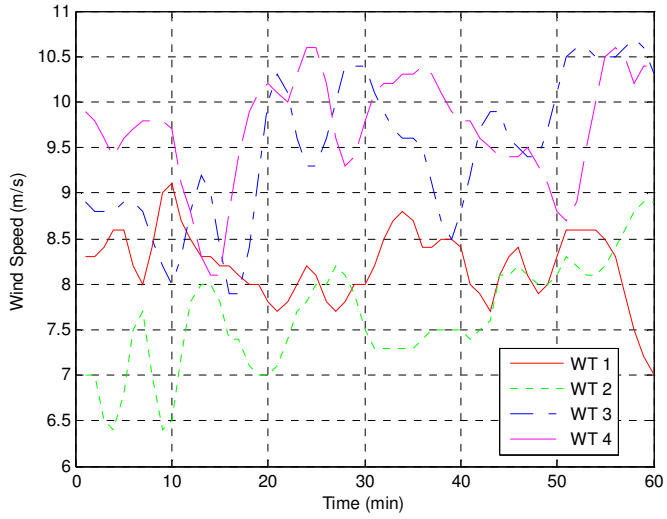

Figure 5.20 – Wind speeds vs. time

In the case of the individual speed control, each turbine would individually adjust its speed to the wind speed of its own based on its own output power. These adjusted speeds are plotted in Figure 5.21. On the other hand, in the centralized speed control method, all the wind turbines in the farm will have approximately the same speed. In this simulation case, this speed is demonstrated in Figure 5.22.

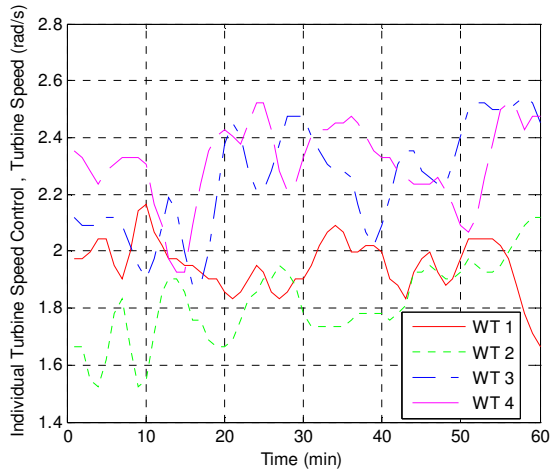

Figure 5.21 – Turbine speeds under individual control vs. time

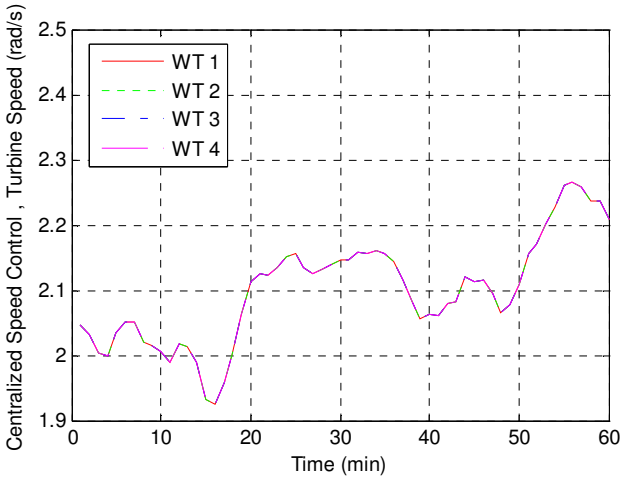

Figure 5.22 – Turbine speeds under centralized control vs. time

This individual speed adjustment would lead to $C_{p,max}$ and the corresponding power for this situation is plotted in Figure 5.23. However, it should be noted that in reality the aerodynamic efficiency will not be $C_{p,max}$ and will be less than that. The power produced by each individual wind turbine in the centralized speed control method is demonstrated in Figure 5.24.

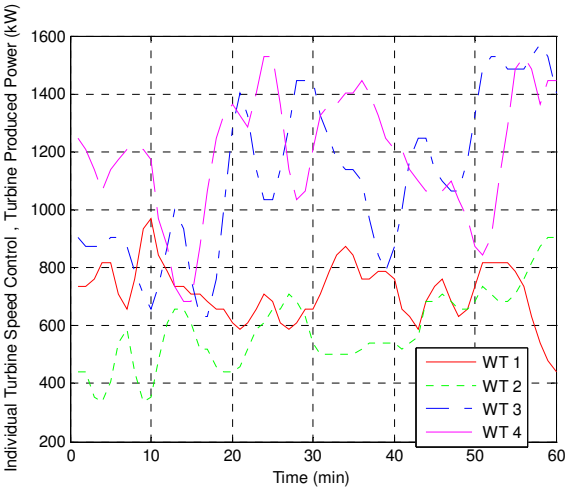

Figure 5.23 – Produced power under individual control vs. time

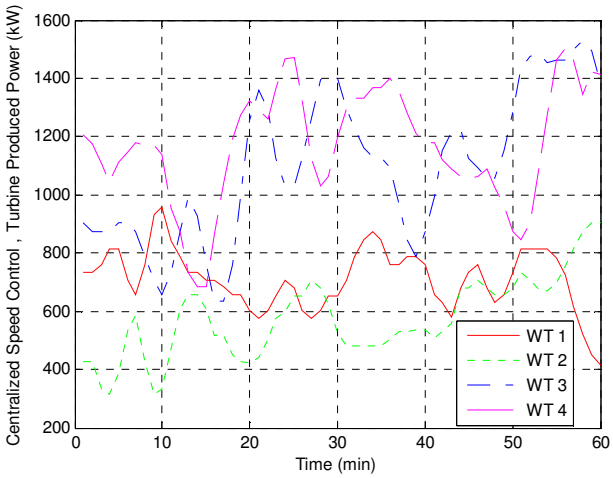

Figure 5.24 – Produced power under centralized control vs. time

Figure 5.25 shows the total power produced by the wind farm in both cases. As is apparent, the removal of the individual speed control system did not make a considerable difference.

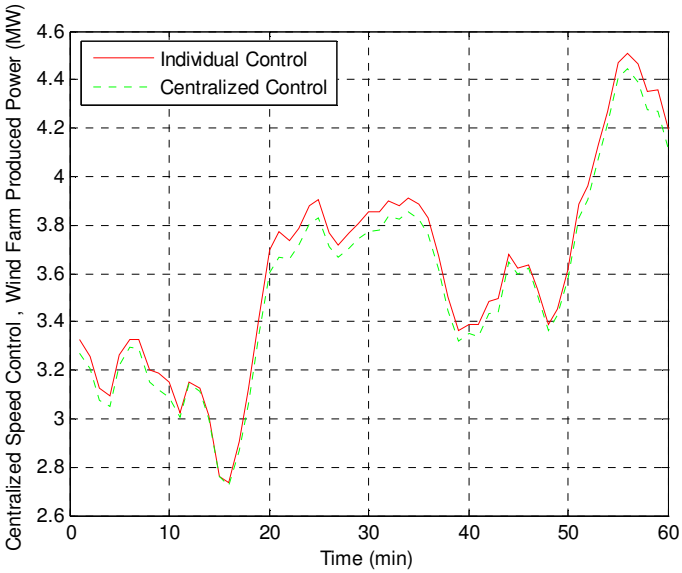

Figure 5.25 – Wind farm produced power vs. time

In order to study this fact more closely, the difference in the produced power in two cases are calculated and plotted in Figure 5.26. Figure 5.27 shows the percentage of the power loss due to the removal of the individual speed control system.

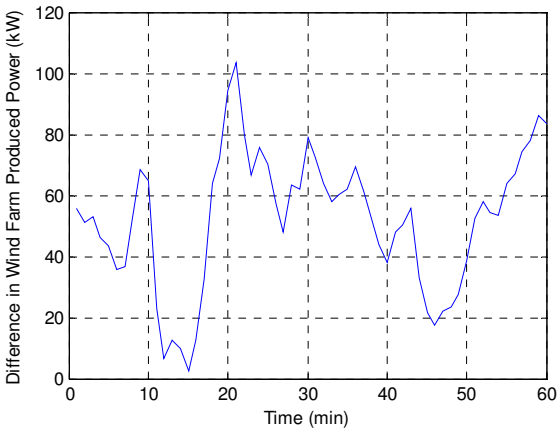

Figure 5.26 – Power loss due to the application of the centralized control vs. time

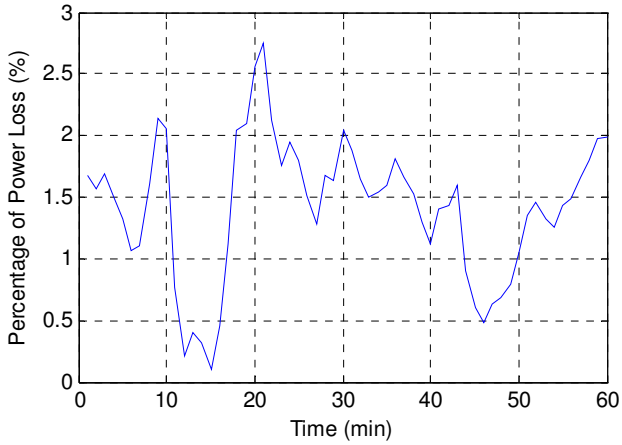

Figure 5.27 – Percentage of the power loss vs. time

Tables 5.10 shows the instantaneous power losses in the centralized control method.

Maximum lost instantaneous power through centralized control	103.6100 kW (2.7464 %)
Average lost instantaneous power through centralized control	52.2190 kW (1.3842 %)

Table 5.10 – Lost instantaneous power through the centralized control method

Table 5.11 shows the produced energy through different methods and the percentage of the energy loss due to the removal of the individual control systems in the wind turbines.

Produced energy through individual control method	3.54 MWh
Produced energy through centralized control method	3.50 MWh
Energy loss through removal of individual control system	1.41 %

Table 5.11 – Produced energy through different methods

It is seen that the removal of individual speed control system does not decrease the efficiency magnificiently and this means that centralized speed control may be an appropriate solution for the future wind farms from an energy efficiency point of view.

Annual energy production analysis

In order to compare the centralized control method with the individual wind turbine control method, the annual operation of a wind farm is studied and the percentage of the energy production losses due to the removal of the individual control and employing the centralized control instead is calculated. The studied wind farm consists of nine wind turbines arranged in a 3x3 configuration. Average wind speed distribution throughout the year is assumed to be the Rayleigh distribution with the mean value equal to the mean wind speed throughout the year. A coefficient depending on the distance between the rows and the speed of the blowing wind accounts for the wake effects. In order to get insight into the concept of the annual energy loss and the hourly energy loss, Table 5.12 should be considered. This table shows the percentage of the energy loss due to the incorrect reference speed setting in a wind turbine. In the case that the actual wind speed at a wind turbine is $\boldsymbol{v_{actual}}$ but the reference speed for the maximization of the aerodynamic conversion process is mistakenly set to $\boldsymbol{v_{incorrect-reference}}$, the percentage of hourly energy loss due to this incorrect reference setting may be obtained.

$$v_{wind,assumed} = v_{actual} \rightarrow \lambda_{max} = \frac{R\omega^*}{v_{actual}} \rightarrow \tag{5.1}$$

$$\omega^* = \frac{\lambda_{max} v_{actual}}{R} \xrightarrow{C_p(\lambda_{max})=C_{p,max}} P_{cor.-ref.} = {}^1\!/_2\, \rho A C_{p,max} {v_{wind}}^3 \tag{5.2}$$

But, if the reference speed is incorrect:

$$v_{wind,assumed} = v_{inc.-ref.} \rightarrow \lambda_{max} = \frac{R\omega^*}{v_{inc.-ref}} \rightarrow \tag{5.3}$$

$$\omega^* = \frac{\lambda_{max} v_{inc.-ref}}{R} \rightarrow \tag{5.4}$$

$$\lambda_{actual} = \frac{R\omega^*}{v_{actual}} = \frac{R}{v_{actual}} \times \frac{\lambda_{max} v_{inc.-ref}}{R} \rightarrow \tag{5.5}$$

$$\lambda_{actual} = \lambda_{max} \frac{v_{inc.-ref}}{v_{actual}} \rightarrow \tag{5.6}$$

$$\%E_{hourly-loss} = \frac{E_{1hr-cor.-ref} - E_{1hr-inc.-ref}}{E_{1hr-cor.-ref.}} \tag{5.7}$$

$$= \frac{P_{cor.-ref} - P_{inc.-ref}}{P_{cor.-ref.}} \rightarrow \tag{5.8}$$

$$\%E_{hourly-loss} = \frac{C_{p,max} - C_{p,inc.-ref.}(\lambda_{actual})}{C_{p,max}} \tag{5.9}$$

Calculations show that the percentage of the hourly energy loss depends only on the percentage of the relative error in the wind speed reference. Table 5.12 demonstrates the percentage of the hourly energy loss vs. the relative error in the reference wind speed.

Relative error in the reference speed (for all reference speeds)	Percentage of hourly energy loss
+ 10 %	0.3572 %
+ 5 %	0.0786 %
0	0 %
- 5 %	0.5528 %
- 10 %	1.7786 %

Table 5.12 – Senstivity analysis of an incorrect reference speed in the efficiency maximization process

It is observed that although the aerodynamic efficiency plays a key role in the amount of the hourly produced energy and in order to maximize the hourly produced energy, the aerodynamic efficiency should be maximized and the rotational speed should be set accordingly, small relative errors in the reference wind speed do not lead to very large amounts of lost energy per hour.

Figure 5.28 demonstrates the case with wind direction 90°.

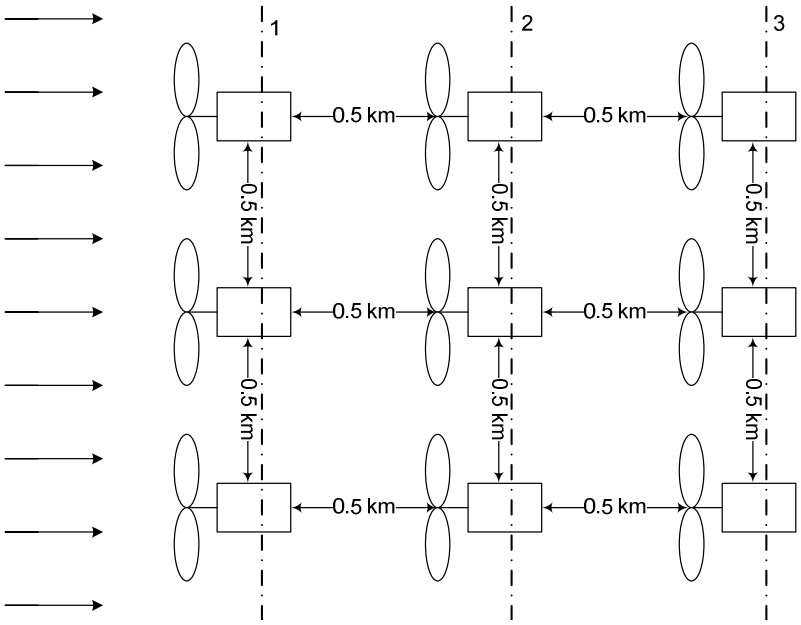

Figure 5.28 - The case setup for the simulation

In this situation, the wind speed is assumed to be blowing normal to the first row of the wind turbines. This means that the average wind speed that the wind turbines in the second and the third rows experience is lower than the wind speed that wind turbines in the first and second rows experience. Table 5.13 demonstrates the percentages of hourly energy losses along with the set of corresponding wind speeds.

Wind Speed Group 1	Wind Speed Group 2	Wind Speed Group 3	Hourly Produced Energy (Individual Control)	Hourly Produced Energy (Centralized control)	Percentage of the Hourly Energy Loss
1.00 m/s	1.00 m/s	1.00 m/s	0.00 MWh	0.00 MWh	**0.00 %**
2.00 m/s	2.00 m/s	2.00 m/s	0.00 MWh	0.00 MWh	**0.00 %**
3.00 m/s	3.00 m/s	3.00 m/s	0.00 MWh	0.00 MWh	**0.00 %**
4.00 m/s	3.46 m/s	3.46 m/s	0.25 MWh	0.25 MWh	**0.00 %**
5.00 m/s	4.32 m/s	3.74m/s	0.79MWh	0.78MWh	**0.56 %**
6.00 m/s	5.19 m/s	4.49 m/s	1.72 MWh	1.69 MWh	**1.71 %**
7.00 m/s	6.06 m/s	5.24 m/s	2.73 MWh	2.68 MWh	**1.71 %**
8.00 m/s	6.92 m/s	5.99 m/s	4.08 MWh	4.01 MWh	**1.71 %**
9.00 m/s	7.79 m/s	6.74 m/s	5.80MWh	5.71 MWh	**1.71 %**
10.00 m/s	8.70 m/s	7.52 m/s	8.03 MWh	7.90 MWh	**1.63 %**
11.00 m/s	9.70 m/s	8.42 m/s	10.94 MWh	10.78 MWh	**1.41 %**
12.00 m/s	10.76 m/s	9.45 m/s	14.71 MWh	14.55 MWh	**1.06 %**
13.00 m/s	11.83 m/s	10.58 m/s	18.15 MWh	18.13 MWh	**0.11 %**
14.00 m/s	12.09 m/s	11.73 m/s	20.61 MWh	20.61 MWh	**0.02 %**
15.00 m/s	13.97 m/s	12.88 m/s	21.60 MWh	21.60 MWh	**0.00 %**
16.00 m/s	15.03 m/s	14.00 m/s	21.60 MWh	21.60 MWh	**0.00 %**
17.00 m/s	16.08 m/s	15.12 m/s	21.60 MWh	21.60 MWh	**0.00 %**
18.00 m/s	17.14 m/s	16.23 m/s	21.60 MWh	21.60 MWh	**0.00 %**
19.00 m/s	18.18 m/s	17.32 m/s	21.60 MWh	21.60 MWh	**0.00 %**
20.00 m/s	19.22 m/s	18.40 m/s	21.60 MWh	21.60 MWh	**0.00 %**

Table 5.13 - Percentage of the hourly energy losses and corresponding wind speeds vs. the blowing incident windfront speed (90° situation)

The percentage of the hourly energy loss has been plotted in Figure 5.29.

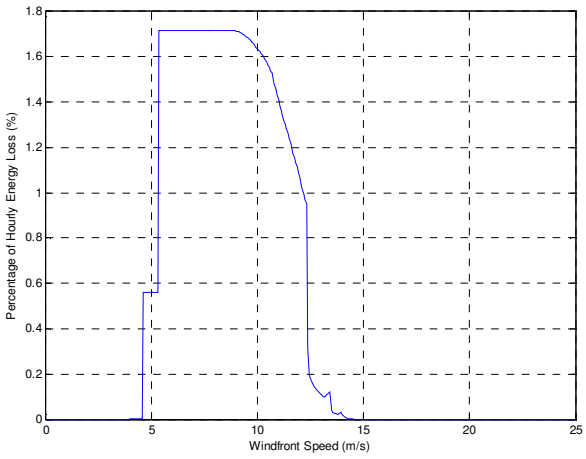

Figure 5.29 - Percentage of the hourly energy losses vs. windfront speed (90° direction)

Table 5.14 demonstrates the percentages of annual energy losses in areas with different average annual wind speeds.

Average Annual Wind Speed	Annual Produced Energy (Individual Control)	Annual Produced Energy (Centralized Control)	Percentage of Annual Energy Loss
1.00 m/s	0.00 GWh	0.00 GWh	**0.00 %**
2.00 m/s	0.87 GWh	0.86 GWh	**0.57 %**
3.00 m/s	9.13 GWh	9.02 GWh	**1.23 %**
4.00 m/s	29.14 GWh	28.71 GWh	**1.47 %**
5.00 m/s	62.53 GWh	61.65 GWh	**1.40 %**
6.00 m/s	108.80 GWh	107.49 GWh	**1.20 %**
7.00 m/s	162.81 GWh	161.22 GWh	**0.97 %**
8.00 m/s	216.70 GWh	214.98 GWh	**0.79 %**
9.00 m/s	263.45 GWh	261.70 GWh	**0.66 %**
10.00 m/s	299.10 GWh	297.41 GWh	**0.57 %**
11.00 m/s	322.80 GWh	321.19 GWh	**0.50 %**
12.00 m/s	335.65 GWh	334.15 GWh	**0.45 %**
13.00 m/s	339.68 GWh	338.29 GWh	**0.41 %**
14.00 m/s	337.03 GWh	335.75 GWh	**0.38 %**
15.00 m/s	329.63 GWh	328.46 GWh	**0.35 %**

Table 5.14 - Percentage of the annual energy losses for different average annual wind speeds (90° situation)

Figure 5.30 demonstrates the percentage of the annual energy loss for different mean annual wind speeds.

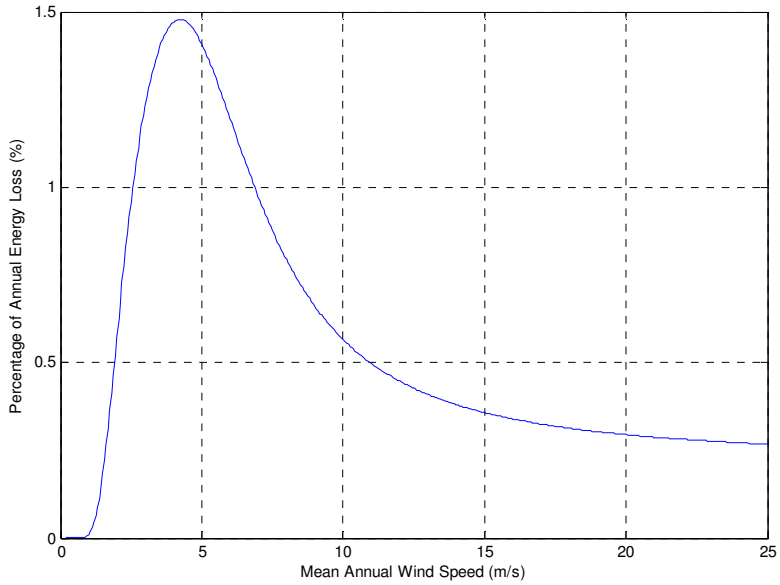

Figure 5.30 - Percentage of the annual energy losses vs. mean annual wind speed (90° situation)

Figure 5.31 demonstrates the case with the wind direction 45°.

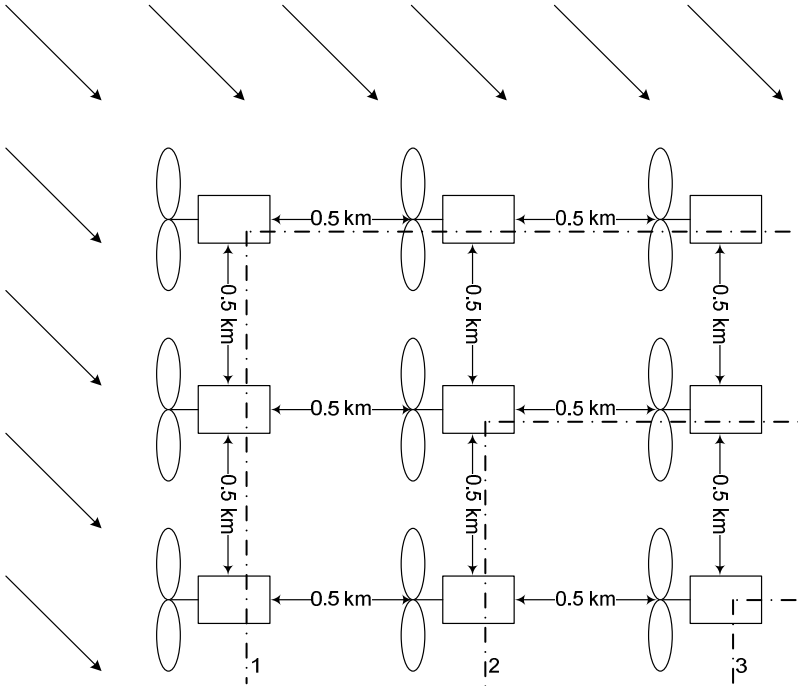

Figure 5.31 - The case setup for the simulation

In this situation, the previous analysis had been done. Table 5.15 demonstrates the percentages of hourly energy losses along with the set of corresponding wind speeds.

Wind Speed Group 1	Wind Speed Group 2	Wind Speed Group 3	Hourly Produced Energy (Individual Control)	Hourly Produced Energy (Centralized control)	Percentage of the Hourly Energy Loss
1.00 m/s	1.00 m/s	1.00 m/s	0.00 MWh	0.00 MWh	**0.00 %**
2.00 m/s	2.00 m/s	2.00 m/s	0.00 MWh	0.00 MWh	**0.00 %**
3.00 m/s	3.00 m/s	3.00 m/s	0.00 MWh	0.00 MWh	**0.00 %**
4.00 m/s	3.46 m/s	3.46 m/s	0.41 MWh	0.41 MWh	**0.00 %**
5.00 m/s	4.32 m/s	3.74 m/s	1.11 MWh	1.10 MWh	**0.45 %**
6.00 m/s	5.19 m/s	4.49 m/s	2.04 MWh	2.02 MWh	**0.83 %**
7.00 m/s	6.06 m/s	5.24 m/s	3.24 MWh	3.21 MWh	**0.83 %**
8.00 m/s	6.92 m/s	5.99 m/s	4.84 MWh	4.80 MWh	**0.83 %**
9.00 m/s	7.79 m/s	6.74 m/s	6.89 MWh	6.83 MWh	**0.83 %**
10.00 m/s	8.70 m/s	7.52 m/s	9.50 MWh	9.43 MWh	**0.79 %**
11.00 m/s	9.70 m/s	8.42 m/s	12.83 MWh	12.73 MWh	**0.72 %**
12.00 m/s	10.76 m/s	9.45 m/s	16.98 MWh	16.87 MWh	**0.62 %**
13.00 m/s	11.83 m/s	10.58 m/s	19.90 MWh	19.89 MWh	**0.07 %**
14.00 m/s	12.90 m/s	11.73 m/s	21.27 MWh	21.27 MWh	**0.00 %**
15.00 m/s	13.97 m/s	12.88 m/s	21.60 MWh	21.60 MWh	**0.00 %**
16.00 m/s	15.03 m/s	14.00 m/s	21.60 MWh	21.60 MWh	**0.00 %**

17.00 m/s	16.08 m/s	15.12 m/s	21.60 MWh	21.60 MWh	**0.00 %**
18.00 m/s	17.14 m/s	16.23 m/s	21.60 MWh	21.60 MWh	**0.00 %**
19.00 m/s	18.18 m/s	17.32 m/s	21.60 MWh	21.60 MWh	**0.00 %**
20.00 m/s	19.22 m/s	18.40 m/s	21.60 MWh	21.60 MWh	**0.00 %**

Table 5.15 - Percentage of the hourly energy losses and corresponding wind speeds (45° situation)

Percentage of the hourly energy loss has been plotted in Figure 5.32.

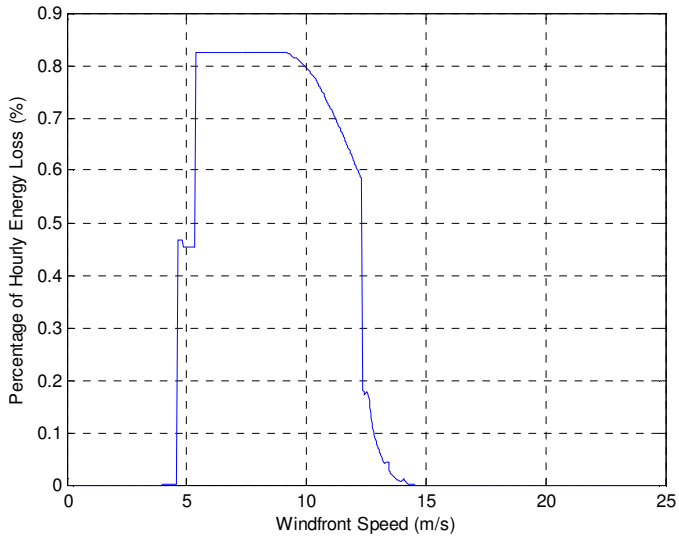

Figure 5.32 - Percentage of the hourly energy losses vs. windfront speed (45° situation)

Table 5.16 demonstrates the percentages of annual energy losses in areas with different average annual wind speeds.

Average Annual Wind Speed	Annual Produced Energy (Individual Control)	Annual Produced Energy (Centralized Control)	Percentage of Annual Energy Loss
1.00 m/s	0.00 GWh	0.00 GWh	**0.00 %**
2.00 m/s	1.28 GWh	1.27 GWh	**0.30 %**
3.00 m/s	11.85 GWh	11.78 GWh	**0.60 %**
4.00 m/s	35.82 GWh	35.56 GWh	**0.71 %**
5.00 m/s	74.58 GWh	74.06 GWh	**0.70 %**
6.00 m/s	126.41 GWh	125.63 GWh	**0.61 %**
7.00 m/s	184.75 GWh	183.70 GWh	**0.51 %**
8.00 m/s	241.19 GWh	240.16 GWh	**0.43 %**
9.00 m/s	288.91 GWh	287.86 GWh	**0.36 %**
10.00 m/s	324.40 GWh	323.37 GWh	**0.31 %**
11.00 m/s	347.21 GWh	346.24 GWh	**0.28 %**
12.00 m/s	358.79 GWh	357.88 GWh	**0.25 %**
13.00 m/s	361.36 GWh	360.51 GWh	**0.23 %**
14.00 m/s	357.21 GWh	356.43 GWh	**0.22 %**
15.00 m/s	348.33 GWh	347.62 GWh	**0.21 %**

Table 5.16 - Percentage of the annual energy losses for different average annual wind speeds (45° situation)

Figure 5.33 demonstrates the percentage of the annual energy loss for different mean annual wind speeds.

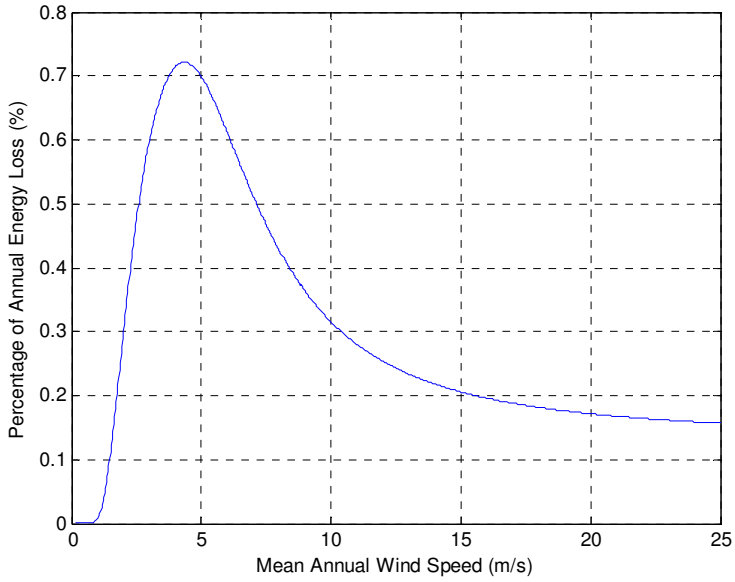

Figure 5.33 - Percentage of the annual energy losses vs. mean annual wind speed (45° situation)

In order to analyze the results, first of all, the percentages of the hourly energy losses versus the incident windfront speeds should be considered in both 90° and 45° situations. The wind turbines begin working at the wind speed 4 m/s. So, obviously below 4 m/s, there is no hourly loss as there is no production at all. Also, between 4 m/s and about 4.3 m/s, there is energy production but there is no hourly energy loss as due to the wake effects at the wind turbines of the first row, the turbines in the next rows do not receive wind speeds high enough to work. This is the reason that there is no hourly energy loss in this wind speed range. In the wind speed range 4.3 m/s ~ 5.3 m/s, there is energy loss but it is much lower than the maximum energy loss and this is due to the fact that only 2 groups out of 3 groups of wind turbines are working. Similar to the last reasoning, the fewer the number of different wind speeds at the site, the less the amount of hourly energy loss. Between 5.3 m/s and about 8 m/s, there is maximum energy loss due to the fact that all the wind turbines are working and moreover they are in a rotational speed range that can have high values of C_p and accordingly, they absorb as much possible wind energy as they can, so, with high values of C_t, the wind speeds at the next group of turbines drop the most in this range. From the end of this range, until about the wind speed 12.3 m/s, the percentage of hourly energy loss decreases continuously. This is due to the fact that above 8 m/s, the C_p and C_t decrease continuously as the wind turbines have reached their rotational speed limit and neither the individual control method nor the centralized control method can adapt the rotational speed to absorb more energy. So, both methods become inefficient. Above 12.3 m/s and until 20 m/s, both control methods produced the same amount of energy as although due to the wake effects, the wind speeds at next groups of turbines have decreased, they are receiving more than maximum

amount of energy that they can absorbed based on the generator power rating. So, at 12.3 m/s, with a steep slope, the energy losses decreases. Moreover, it is observed that in the 45° situation, the percentage of the hourly energy loss is generally lower than in the 90° situation. This is due to fact that in the first situation 5 out of 9 turbines receive the same wind speed, and then 3 out of 9 turbines receive nearly the same speed but in the second situation only 3 groups of 3 turbines receive the same wind speed. So, in general, in the first situation more number of the wind turbines are receiving the same wind speed and based on the fact that the efficiency of the centralized control method depends on the values of the wind speeds being near each other, one may conclude that generally the 45° degree situation has less energy loss due to the removal of the individual speed control systems. It is observed that even in the worst case, the percentage of losses due to the replacement of the individual speed control system with the centralized control system is less than 2%. Therefore, from an energy efficiency point of view, one may conclude that employing a centralized control strategy will not lead to large amount of energy losses.

6. Conclusion

To sum up, it is concluded that in the offshore wind farms where an HVDC transmission is used, it is possible to remove the individual control systems along with the corresponding converters and replace them with a single larger converter in the HVDC station. In this case, a more advanced control strategy should be used for controlling the converter in the HVDC station. In this thesis work, it is shown that it is possible to derive a centralized control strategy. The control strategy that the controller follows should involve the maximization of the energy absorbed from the wind by the wind turbines through setting the correct reference grid frequency and thus the correct reference rotational speed for the whole wind farm and also compensate for the slip so that the aerodynamic efficiencies become maximum and also may involve minimizing the lost energy by increasing the efficiencies through setting the correct reference voltage level. It is shown in this work that the energy input to the wind turbine can be maximized by setting a correct rotational speed as the reference and the lost energy in the system can be minimized by lowering the flux magnitude at low wind speeds. It is also shown that in addition to being feasible, the percentage of the annual lost energy due to using this centralized strategy is less than 2% in the worst case and moreover such losses decrease in the areas where the wind is less gusty.

Appendix A: Wind turbine data

In order to perform the simulations for this thesis work, a prototype generator designed for wind turbines manufactured by ABB was used. Also, the corresponding wind turbine was used whose information will come later. The specifications for the equivalent circuit of this generator and the wind turbine are:

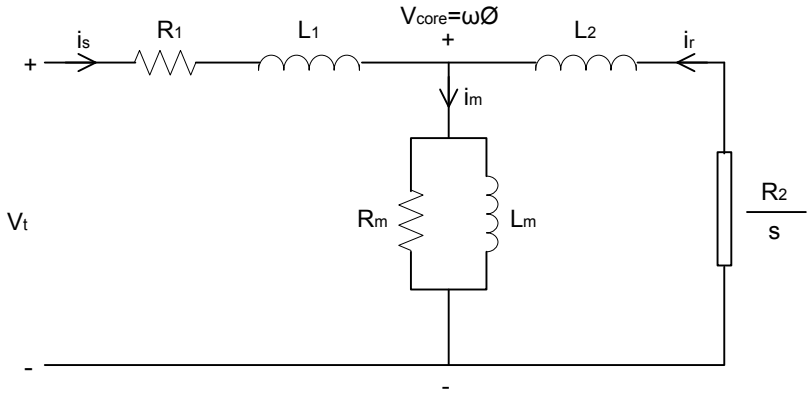

Figure A.1 – Equivalent circuit of the wind turbine generator

$P_{rated} = 2.4\ MW$
$V_{rated} = 750\ V$
$I_{rated} = 2039\ A$
$(\cos\varphi)_{rated} = 0.91$
$R_s = 0.0014\ \Omega$
$R_r = 0.0013\ \Omega$
$X_{s\lambda} = 0.0262\ \Omega$
$X_{r\lambda} = 0.0191\ \Omega$
$X_m = 0.79\ \Omega$
$R_m = 38\ \Omega$
$J_g = 53.036\ kg.m^2$
$n_p = 2$
$n_{rated} = 1509\ rpm$
$J_b = 2{,}997{,}044\ kg.m^2$
$v_{cut-in} = 4\ ^m/_s$
$v_{cut-out} = 20\ ^m/_s$
$n_{max} = 20.36\ rpm$
$R = 37\ m$
$k_{sp} = 0.59\ ^{G.Nm}/_s$
$k_d = 10\ ^{M.Nm}/_s$
$v_{wind,rated} = 12.3\ ^m/_s$

$C_p - \beta, \lambda$ surface comes as the following:

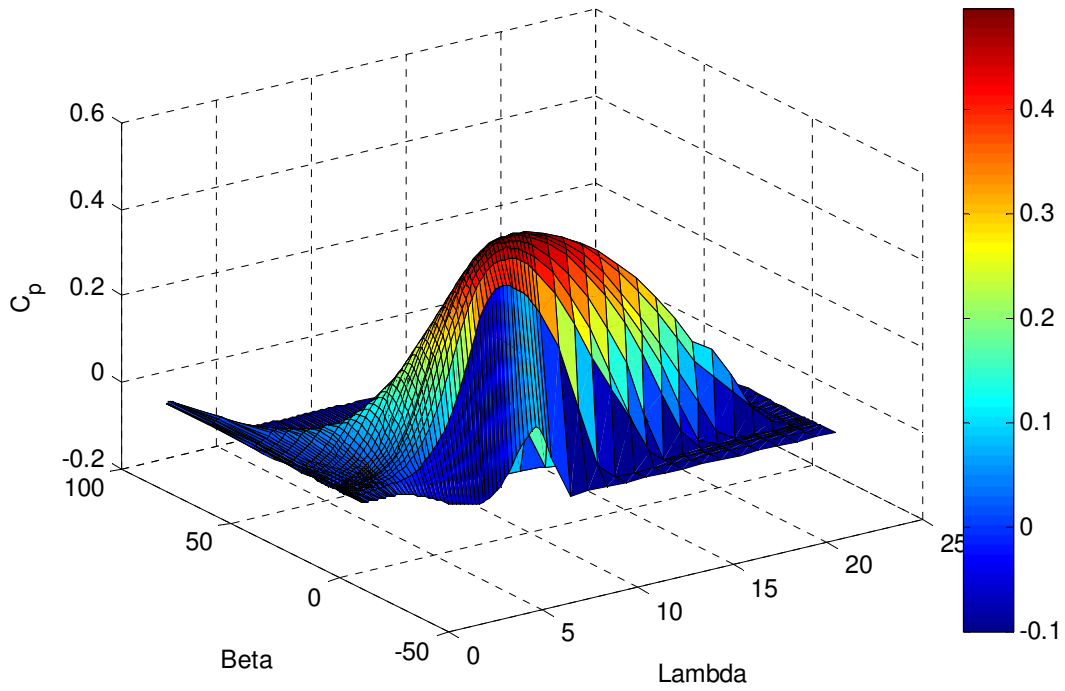

Figure A.2 - $C_p - \beta, \lambda$ surface for the wind turbine

$C_p - \lambda$ curve for the turbine comes as the following:

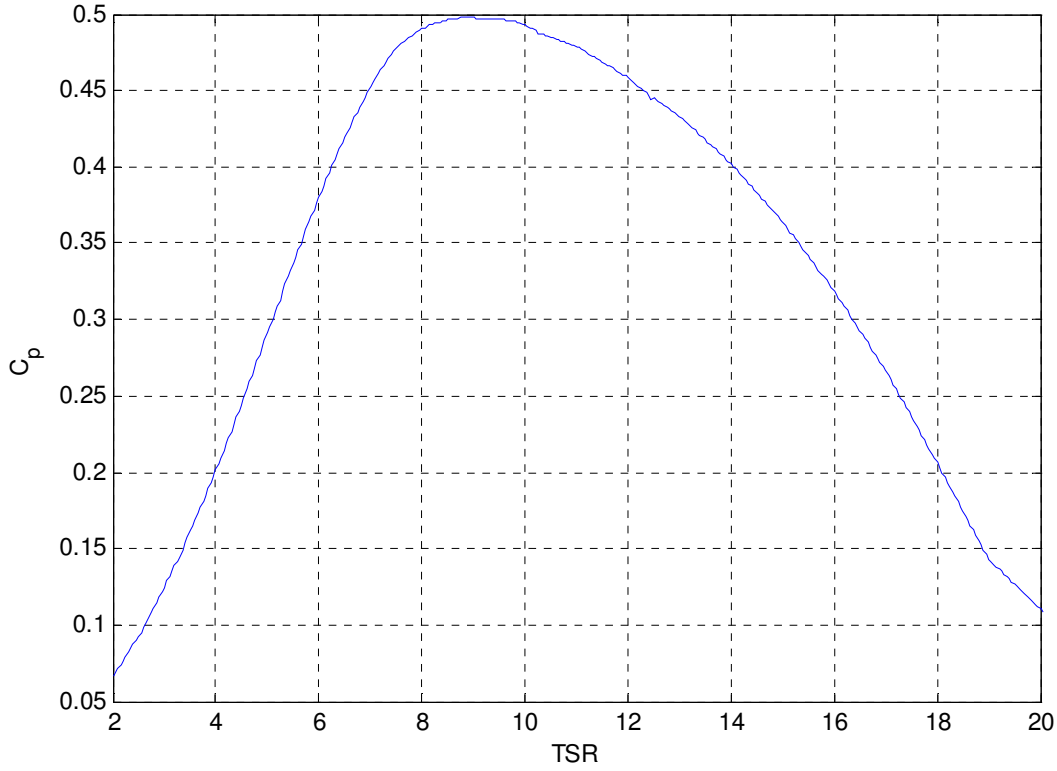

Figure A.3 - $C_p - \lambda$ curve for the wind turbine

β – λ lookup graph and table come as the following:

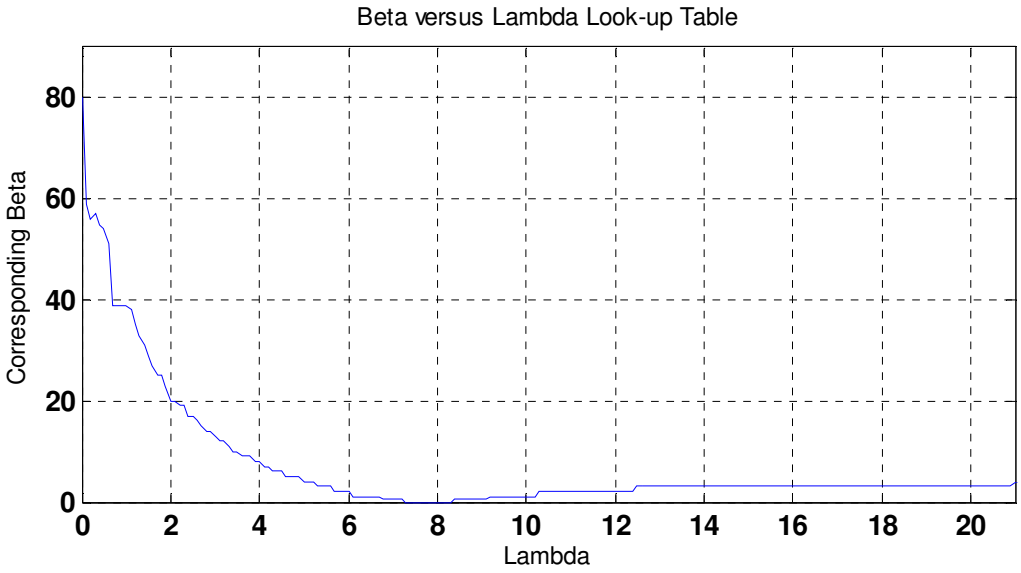

Figure A.4 – Pitch angle values vs. the tip speed ratio

λ	β	λ	B	λ	β	Λ	β	λ	β	λ	β	λ	β	λ	β
0	80	3	13	6	2	8.9	0.4667	11.9	2	14.9	3	17.9	3	20.9	3
0.1	59	3.1	12	6.1	1	9	0.4667	12	2	15	3	18	3	21	4
0.2	56	3.2	12	6.2	1	9.1	0.4667	12.1	2	15.1	3	18.1	3	21.1	4
0.3	57	3.3	11	6.3	1	9.2	1	12.2	2	15.2	3	18.2	3	21.2	4
0.4	55	3.4	10	6.4	1	9.3	1	12.3	2	15.3	3	18.3	3	21.3	4
0.5	54	3.5	10	6.5	1	9.4	1	12.4	2	15.4	3	18.4	3	21.4	4
0.6	51	3.6	9	6.6	1	9.5	1	12.5	3	15.5	3	18.5	3	21.5	4
0.7	39	3.7	9	6.7	1	9.6	1	12.6	3	15.6	3	18.6	3		
0.8	39	3.8	9	6.8	0.4667	9.7	1	12.7	3	15.7	3	18.7	3		
0.9	39	3.9	8	6.9	0.4667	9.8	1	12.8	3	15.8	3	18.8	3		
1	39	4	8	7	0.4667	9.9	1	12.9	3	15.9	3	18.9	3		
1.1	38	4.1	7	7.1	0.4667	10	1	13	3	16	3	19	3		
1.2	35	4.2	7	7.2	0.4667	10.1	1	13.1	3	16.1	3	19.1	3		
1.3	33	4.3	6	7.3	0	10.2	1	13.2	3	16.2	3	19.2	3		
1.4	31	4.4	6	7.4	0	10.3	2	13.3	3	16.3	3	19.3	3		
1.5	29	4.5	6	7.5	0	10.4	2	13.4	3	16.4	3	19.4	3		
1.6	27	4.6	5	7.6	0	10.5	2	13.5	3	16.5	3	19.5	3		
1.7	25	4.7	5	7.7	0	10.6	2	13.6	3	16.6	3	19.6	3		
1.8	25	4.8	5	7.8	0	10.7	2	13.7	3	16.7	3	19.7	3		
1.9	23	4.9	5	7.9	0	10.8	2	13.8	3	16.8	3	19.8	3		
2	20	5	4	8	0	10.9	2	13.9	3	16.9	3	19.9	3		
2.1	20	5.1	4	8.1	0	11	2	14	3	17	3	20	3		
2.2	19	5.2	4	8.2	0	11.1	2	14.1	3	17.1	3	20.1	3		
2.3	19	5.3	3	8.3	0	11.2	2	14.2	3	17.2	3	20.2	3		

2.4	17	5.4	3	8.4	0.4667	11.3	2	14.3	3	17.3	3	20.3	3		
2.5	17	5.5	3	8.5	0.4667	11.4	2	14.4	3	17.4	3	20.4	3		
2.6	16	5.6	3	8.6	0.4667	11.5	2	14.5	3	17.5	3	20.5	3		
2.7	15	5.7	2	8.7	0.4667	11.6	2	14.6	3	17.6	3	20.6	3		
2.8	14	5.8	2	8.8	0.4667	11.7	2	14.7	3	17.7	3	20.7	3		
2.9	14	5.9	2	8.85	0.4667	11.8	2	14.8	3	17.8	3	20.8	3		

Table A.1 – Pitch angle look-up table

References

[1] S. Lundberg, “Wind Farm Configuration and Energy Efficiency Studies”, PhD Thesis, Chalmers University of Technology, Göteborg, Sweden, 2006.

[2] S. Lundberg, “Conguration study of large wind parks”, Licenciate Thesis, Chalmers University of Technology, Göteborg, Sweden, 2003.

[3] L. Max, “Energy Evaluation for DC/DC Converters in DC-Based Wind Farms”, Licenciate Thesis, Chalmers University of Technology, Göteborg, Sweden, 2007.

[4] S. Lundberg, “Evaluation of Wind Farm Layouts”, Nordic Workshop on Power and Industrial Electronics, 2004.

[5] S. Lundberg and O. Carlsson, “Integration of Wind Power by DC-Power Systems”, IEEE PowerTech, St. Petersburg, Russia, June 27-30, 2005.

[6] D. A. Spera, “Wind Turbine Technology”, ASME Press, 1994.

[7] Danish Wind Industry Association, “WindPower.org”, Denmark, 2003.

[8] C. B. Hasager, P. Astrup, M. B. Christiansen, M. Nielsen and R. Barthelmie, “Wind resources and wind farm wake effects offshore observed from satellite”, European Wind Energy Conference, Germany, February 2006.

[9] R. J. Barthelmie and others, “Modelling and measurements of wakes in large wind farms”, Journal of Physics, Conference Series 75, 2007.

[10] A. Lewinschal, “A Simple Method for Calculations of Wake Effects in Wind Farms with Influence of Atmospheric Stability”, ISSN 1650-6553 Nr. 157, MSc Thesis, Uppsala University, Sweden, 2008.

[11] M. O. L. Hansen, “Aerodynamics of Wind Turbines: Rotors, Loads and Structure”, James & James (Science Publishers) Ltd., ISBN 1902916069, London, 2001.

[12] R. J. Barthelmie, M. S. Courtney, J. Højstrup and P. Sanderhoff, “The Vindeby Project”, Report Risö-R-741 (EN), Risö National Laboratory, Denmark, 1994.

[13] P. Rosas, “Dynamic Influences of Wind Power on the Power System”, PhD Thesis, Technical University of Denmark (D.T.U.), Denmark, March 2003.

[14] K. Rudion, “Aggregated modelling of wind farms", PhD Thesis, Otto-von-Guericke-Universitäat Magdeburg, Magdeburg, Germany, February 2008.

[15] A. Perdana, “Dynamic Models of Wind Turbines”, PhD Thesis, Chalmers University of Technology, Göteborg, Sweden, 2009.